

Sampling from Bayesian Neural Network Posteriors with Symmetric Minibatch Splitting Langevin Dynamics

Daniel Paulin^{1,*}, Peter A. Whalley^{2,*}, Neil K. Chada³, and Benedict Leimkuhler¹

¹University of Edinburgh, Edinburgh, UK

²Seminar for Statistics, ETH Zürich, Zürich, Switzerland

³City University of Hong Kong, Hong Kong SAR

*Both authors contributed equally to this work

October 29, 2024

Abstract

We propose a scalable kinetic Langevin dynamics algorithm for sampling parameter spaces of big data and AI applications. Our scheme combines a symmetric forward/backward sweep over minibatches with a symmetric discretization of Langevin dynamics. For a particular Langevin splitting method (UBU), we show that the resulting Symmetric Minibatch Splitting-UBU (SMS-UBU) integrator has bias $\mathcal{O}(h^2 d^{1/2})$ in dimension $d > 0$ with stepsize $h > 0$, despite only using one minibatch per iteration, thus providing excellent control of the sampling bias as a function of the stepsize. We apply the algorithm to explore local modes of the posterior distribution of Bayesian neural networks (BNNs) and evaluate the calibration performance of the posterior predictive probabilities for neural networks with convolutional neural network architectures for classification problems on three different datasets (Fashion-MNIST, Celeb-A and chest X-ray). Our results indicate that BNNs sampled with SMS-UBU can offer significantly better calibration performance compared to standard methods of training and stochastic weight averaging.

1 Introduction

Bayesian neural networks (BNNs) are a statistical paradigm which has been widely advocated to improve the reliability of neural networks by formulating questions regarding parameter sensitivity and prediction error in terms of the structure of the posterior parameter distribution. The ultimate goals of BNNs (already espoused in the seminal works of [44] and [40]) are to reduce generalization error and enhance robustness of trained models. Due to the capacity of BNNs to quantify uncertainty, they have been proposed for use in applications such as astronomy, and modelling partial differential equations ([19], [25]), but their potential impact is much greater and includes topics in data-driven engineering ([39], [56]) and automated medical diagnosis ([5], [33]).

While reliance on a Bayesian statistics approach provides theoretical foundation for BNNs, the extreme cost of treating these models has hampered uptake in practical applications. In the modern era, datasets are often very large—a single epoch (pass through the training data) with computation of likelihoods for a large scale network may take hours or days ([55]). Optimization schemes can robustly use efficient data subsampling, whereas BNNs require a more delicate approach, since the target distribution of the Markov chain is easily corrupted ([13], [17], [62]). Scalable alternatives to MCMC based on Gaussian approximation can lead to some improvements in calibration ([41], [8]), but they lack theoretical justification.

The high computational cost of deep learning is also a consequence of the size of the model parameter space, which may consist of many millions (or even billions) of parameters. Sampling the parameters of such models undeniably adds substantial overload in comparison to optimization,

which is already seen as costly, thus a central impediment to exploiting the promise of BNNs is the need for optimal sampling strategies that scale well both in terms of the size of the dataset and parameter space dimension ([22], [32]). The most popular schemes for high dimensional inference are Markov chain Monte Carlo (MCMC) methods ([2]), e.g. Hamiltonian Monte Carlo (HMC) and the Metropolis-adjusted Langevin algorithm (MALA) ([6], [13], [27]), with HMC typically favored in the large scale BNN setting ([30], [47]).

In this article, we present the use of an “unadjusted” sampling scheme, within BNNs, which avoids the costly Metropolis test and is based on the use of efficient symmetric splitting methods for kinetic Langevin dynamics, in particular the UBU discretization, providing second order accuracy in the strong (pathwise) sense and in terms of sampling bias. We show that the second order accuracy can be maintained in combination with a carefully organized minibatch subsampling strategy resulting in a fully symmetric (SMS-UBU) integrator, which provides both efficiency for large datasets and low bias, asymptotically, at high dimension. We implement this scheme for BNNs and demonstrate the performance in comparison with some alternative methods. Numerical tests are conducted using suitable NNs on a range of classification problems involving image data (the fashion-MNIST dataset ([60]), celeb-A dataset ([61]) and a chest X-ray dataset ([31])). To assess the results, we rely on well-known metrics, namely accuracy, negative log-likelihood on test data, adaptive calibration error, and ranked probability score. Our experiments clearly demonstrate the effectiveness of BNNs trained with SMS-UBU compared to standard training and stochastic weight averaging.

The main contributions of this work are: (i) the presentation of a kinetic Langevin scheme incorporating symmetric minibatch subsampling (SMS-UBU) and the demonstration of its second order accuracy, the first result of its kind for a stochastic gradient scheme, (ii) novel bias bounds for vanilla stochastic gradient kinetic Langevin dynamics as a function of dataset size, considering also the control of the bias for minibatches of the dataset drawn without replacement, and (iii) a demonstration of the use of a Bayesian UQ framework for NNs by applying our efficient methods to sample BNNs near targeted posterior modes.

The results are organized as follows: Section 2 gives an overview of kinetic Langevin integrators, while the SMS-UBU schemes appears in Section 2.3 along with a summary of the key theoretical results. Our main theorem is given in Section 3. Section 4 takes up discussion of uncertainty quantification in neural networks, followed by the presentation of classification experiments in Section 5. We conclude in Section 6. Detailed proofs are provided in the supplement, along with additional details about the experiments.

2 Methodology

In this section, we first review sampling through kinetic Langevin integrators. We begin with a brief overview, before discussing a particular splitting order scheme, which is UBU. We will then discuss the extension of UBU to stochastic gradients before introducing our new method which we refer to as SMS-UBU, which is presented in algorithmic form.

2.1 Kinetic Langevin dynamics and discretizations

Denote by $\pi(dx)$ the target probability measure of form $\pi(dx) \propto \exp(-f(x))dx$, where $f(x)$ refers to the potential function. Kinetic Langevin dynamics is the system

$$\begin{aligned} dX_t &= V_t dt, \\ dV_t &= -\nabla f(X_t)dt - \gamma V_t dt + \sqrt{2\gamma}dW_t, \end{aligned} \tag{2.1}$$

on \mathbb{R}^{2d} , where $\{W_t\}_{t \geq 0}$ is a standard d -dimensional Wiener process, and $\gamma > 0$ is a friction coefficient. Under standard assumptions (see [49]), the unique invariant measure of the process $\{X_t, V_t\}_{t \geq 0}$ has density given by

$$\bar{\pi}(dx, dv) \propto \exp\left(-f(x) - \frac{\|v\|^2}{2}\right) dx dv = \pi(dx) \exp\left(-\frac{\|v\|^2}{2}\right) dv, \tag{2.2}$$

with respect to Lebesgue measure. Due to the product form of the invariant measure, averages with respect to the target measure $\pi(dx)$ can be obtained as the configurations generated by approximating paths of (2.1).

Bias in the invariant measure arises, principally, due to two factors: (i) finite stepsize discretization of (2.1), and (ii) the use of stochastic gradients. The choice of integrator, the stepsize, and the friction γ all affect both the convergence rate and the discretization bias ([9], [35], [27]), and this is further altered by the procedure used to estimate the gradient. While the simplest procedure is to use the Euler-Mayurama scheme for the overdamped form of (2.1), together with stochastic gradients (SG), as in the SG-HMC algorithm of [13], there has been significant amount of progress in the numerical analysis community in the development of accurate second order integrators for the kinetic Langevin dynamics (2.1), see [35], [51] and [1]. Here we extend some of these integrators via the use of stochastic gradients.

An accurate splitting method was introduced in [1] and further studied in [51] and [10]. This splitting method only requires one gradient evaluation per iteration but has strong order two. The method is based on breaking up the SDE (2.1) as follows

$$\begin{pmatrix} dX_t \\ dV_t \end{pmatrix} = \underbrace{\begin{pmatrix} 0 \\ -\nabla f(X_t)dt \end{pmatrix}}_{\mathcal{B}} + \underbrace{\begin{pmatrix} V_t dt \\ -\gamma V_t dt + \sqrt{2\gamma}dW_t \end{pmatrix}}_{\mathcal{U}},$$

where each part can be integrated exactly over a step of size h . Given $\gamma > 0$, let $\eta = \exp(-\gamma h/2)$, and for ease of notation, define the following operators

$$\mathcal{B}(x, v, h) = (x, v - h\nabla f(x)), \quad (2.3)$$

and

$$\begin{aligned} \mathcal{U}(x, v, h/2, \xi^{(1)}, \xi^{(2)}) &= \left(x + \frac{1-\eta}{\gamma}v + \sqrt{\frac{2}{\gamma}} \left(\mathcal{Z}^{(1)}(h/2, \xi^{(1)}) - \mathcal{Z}^{(2)}(h/2, \xi^{(1)}, \xi^{(2)}) \right), \right. \\ &\quad \left. \eta v + \sqrt{2\gamma} \mathcal{Z}^{(2)}(h/2, \xi^{(1)}, \xi^{(2)}) \right), \end{aligned} \quad (2.4)$$

where

$$\begin{aligned} \mathcal{Z}^{(1)}(h/2, \xi^{(1)}) &= \sqrt{\frac{h}{2}}\xi^{(1)}, \\ \mathcal{Z}^{(2)}(h/2, \xi^{(1)}, \xi^{(2)}) &= \sqrt{\frac{1-\eta^2}{2\gamma}} \left(\sqrt{\frac{1-\eta}{1+\eta}} \cdot \frac{4}{\gamma h} \xi^{(1)} + \sqrt{1 - \frac{1-\eta}{1+\eta}} \cdot \frac{4}{\gamma h} \xi^{(2)} \right), \end{aligned} \quad (2.5)$$

and $\xi^{(1)}, \xi^{(2)} \sim \mathcal{N}(0_d, I_d)$ are d -dimensional standard Gaussian random variables.

The UBU scheme consists of applying first a half-step (h replaced by $h/2$) using (2.4), then applying an impulse based on the potential energy term, followed by another half-step of the mapping \mathcal{U} . The symmetry of this scheme plays a role in its accuracy, since it causes a cancellation of the first order term in the error expansion.

Other symmetric splitting methods are possible and have been extensively studied in recent years. In particular the BAOAB, ABOBA and OBABO schemes ([9], [35], [36]) are all second order in the weak (sampling bias) sense and make plausible candidates for BNN sampling. In these methods, we further divide the \mathcal{U} stage of the UBU algorithm into two parts and intersperse the resulting solution maps with \mathcal{B} steps to form a numerical scheme. Several of these methods will be compared in Section 5.

2.2 Stochastic gradient algorithms

We first abstractly define stochastic gradients as unbiased estimators of the gradient of the potential, under the same set of assumptions as [37].

Definition 1. A stochastic gradient approximation of a potential f is defined by a function $\mathcal{G} : \mathbb{R}^d \times \Omega \rightarrow \mathbb{R}^d$ and a probability distribution ρ on a Polish space Ω , such that for every $x \in \mathbb{R}^d$, $\mathcal{G}(x, \cdot)$ is measurable on (Ω, \mathcal{F}) , and for $\omega \sim \rho$,

$$\mathbb{E}(\mathcal{G}(x, \omega)) = \nabla f(x).$$

The function \mathcal{G} and the distribution ρ together define the stochastic gradient, which we denote as (\mathcal{G}, ρ) .

The following assumption is useful for controlling the accuracy of the stochastic gradient approximations.

Assumption 1. The Jacobian of the stochastic gradient \mathcal{G} , $D_x \mathcal{G}(x, \omega)$ exists and is measurable on (Ω, \mathcal{F}) . There exists a bound $C_G > 0$ such that, for $\omega \sim \rho$,

$$\sup_{x \in \mathbb{R}^d} \mathbb{E} \|D_x \mathcal{G}(x, \omega) - \nabla^2 f(x)\|^2 \leq C_G.$$

Assumption 2 (Moments of Stochastic Gradient). Let $\mathcal{D}(y, \omega) := \mathcal{G}(y, \omega) - \nabla f(y)$, for all $y \in \mathbb{R}^d$ be the difference between the stochastic gradient approximation, $\mathcal{G}(y, \omega)$, and the true gradient. The following moment bound holds on \mathcal{D}

$$\mathbb{E} [\|\mathcal{D}(y, \omega)\|^2 | y] \leq C_{SG}^2 M^2 \|y - x^*\|^2.$$

In Bayesian inference settings, stochastic gradients are usually considered for a potential $f : \mathbb{R}^d \rightarrow \mathbb{R}$ of the form

$$f(x) = f_0(x) + \sum_{i=1}^{N_D} f_i(x), \quad (2.6)$$

where $x \in \mathbb{R}^d$ and N_D is the size of the dataset; the individual contributions arise as terms in a summation that defines the log-likelihood of parameters given the data. In many applications, such as the ones we consider in this work, both the dimension d and the size of the dataset N_D are large. As a result, gradient evaluations of the potential can be computationally expensive. As a consequence, a stochastic approximation of the gradient is typically used (see e.g. [50]) which dramatically reduces the computational cost by relying only on a sample of the dataset of size $N_b \ll N_D$. For MCMC sampling it is natural to seek a similar approach to improve the scalability ([58], [45]). Within (2.6), f_0 can be chosen to be the negative log density of the prior distribution. Then random variables of the form $\omega \in [N_D]^{N_b}$ are constructed as uniform draws on $[N_D] = \{1, \dots, N_D\}$, taken i.i.d. with replacement ([3]). At each step one uses an unbiased estimator of (2.6) instead of the full gradient evaluation, for example

$$\mathcal{G}(x, \omega | \hat{x}) = \nabla f_0(x) + \sum_{i=1}^{N_D} \nabla f_i(\hat{x}) + \frac{N_D}{N_b} \sum_{i \in \omega} [\nabla f_i(x) - \nabla f_i(\hat{x})], \quad (2.7)$$

such that $\mathbb{E}(\mathcal{G}(x, \omega)) = \nabla f(x)$, where, in case the potential is convex, \hat{x} can be chosen as the minimizer of f , $x^* \in \mathbb{R}^d$. We define the random variables

$$\begin{aligned} Z^x &:= \sqrt{\frac{2}{\gamma}} \left(\mathcal{Z}^{(1)} \left(h/2, \xi^{(1)} \right) - \mathcal{Z}^{(2)} \left(h/2, \xi^{(1)}, \xi^{(2)} \right) \right), \\ Z^v &:= \sqrt{2\gamma} \mathcal{Z}^{(2)} \left(h/2, \xi^{(1)}, \xi^{(2)} \right), \end{aligned} \quad (2.8)$$

based on (2.5). In Algorithm 1 we formulate a stochastic gradient implementation of the UBU scheme.

A limitation of using stochastic gradients is that it can introduce additional bias. In particular, using the standard stochastic gradient approximation (sampling the minibatches i.i.d. at each iteration) reduces the strong order of a numerical integrator for kinetic Langevin dynamics to

Algorithm 1 Stochastic Gradient UBU (SG-UBU)

Initialize $(x_0, v_0) \in \mathbb{R}^{2d}$, stepsize $h > 0$ and friction parameter $\gamma > 0$.

for $k = 1, 2, \dots, K$ **do**

 Sample $Z_k^x, Z_k^v, \tilde{Z}_k^x, \tilde{Z}_k^v$ according to (2.8)

 (U) $(x, v) \rightarrow (x_{k-1} + \frac{1-\eta^{1/2}}{\gamma}v_{k-1} + Z_k^x, \eta^{1/2}v_{k-1} + Z_k^v)$

 Sample $\omega_k \sim \rho$

 (B) $v \rightarrow v - h\mathcal{G}(x, \omega_k)$

 (U) $(x_k, v_k) \rightarrow (x + \frac{1-\eta^{1/2}}{\gamma}v + \tilde{Z}_k^x, \eta^{1/2}v + \tilde{Z}_k^v)$

end for

Output: Samples $(x_k)_{k=0}^K$.

$O(h^{1/2})$. SG-UBU for example will be order 1/2, a dramatic reduction in accuracy compared to its full gradient counterpart (which has strong order two (see [1] and [51])). In terms of the weak order and bias in empirical averages stochastic gradients reduce the order of accuracy in the stepsize from two to one ([57], [54]).

A consequence of the reduced accuracy with respect to stepsize is substantially worse non-asymptotic guarantees and scaling in terms of dimension ([12], [20], [27]).

2.3 Symmetric Minibatch Splitting UBU (SMS-UBU)

We now introduce an alternative stochastic gradient approximation method that relies on a random partition $\omega_1, \dots, \omega_{N_m}$ of $[N_D] = \{1, \dots, N_D\}$, each of size N_b (i.e. they are sampled uniformly without replacement from $[N_D]$, and $\omega_1 \cup \dots \cup \omega_{N_m} = [N_D]$). Then we propose to take UBU steps with gradient approximations using the index-set ω_1 first, then ω_2 all the way up to ω_{N_m} . We follow this with the same sequence of minibatches taken in reverse order. We illustrate this methodology for the UBU integrator below:

$$\underbrace{(\mathcal{UB}_{\omega_1}\mathcal{U})}_{\text{minibatch 1}} \underbrace{(\mathcal{UB}_{\omega_2}\mathcal{U})}_{\text{minibatch 2}} \dots \underbrace{(\mathcal{UB}_{\omega_{N_m}}\mathcal{U})}_{\text{minibatch } N_m} \underbrace{(\mathcal{UB}_{\omega_{N_m}}\mathcal{U})}_{\text{minibatch } N_m} \underbrace{(\mathcal{UB}_{\omega_{N_m-1}}\mathcal{U})}_{\text{minibatch } N_m-1} \dots \underbrace{(\mathcal{UB}_{\omega_1}\mathcal{U})}_{\text{minibatch 1}},$$

where

$$\mathcal{B}_{\omega_l}(x, v, h) = \left(x, v - hN_m \sum_{i \in \omega_l} \nabla f_i(x) \right),$$

and $N_m := N_D/N_b$ is the number of minibatches. We mention that of course this is not specific to the UBU integrator and can be applied to any kinetic Langevin dynamics integrator. However, we detail precisely the SMS stochastic gradient algorithm for the UBU integrator in Algorithm 2.

A motivation for such a splitting is that it ensures that the integrator is symmetric as an integrator along a longer time horizon $T = 2hN_m$ and therefore has improved weak order properties [36]. It also turns out it gains improved strong order properties, which we make rigorous in the following sections.

Remark 1. A similar minibatch selection procedure was used within the context of HMC to integrate Hamiltonian dynamics based on symmetric splitting with gradient approximations for each leapfrog step ([17]). Their motivation was different than ours: they required an integrator for Hamiltonian dynamics for use within HMC, offering high acceptance rate within a Metropolis-Hastings accept/reject step. They did not address the use of this type of subsampling in the unadjusted Langevin setting or consider the potential for improved order of accuracy of such a method. Moreover, they did not consider using different batches across iterations of the algorithm and instead only considered taking samples after a complete forward/backward sweep when the Metropolis-Hastings step was applied. Thus their approach requires an evaluation of the entire dataset between consecutive samples, which is not the case for us in the unadjusted Langevin setting.

Algorithm 2 Symmetric Minibatch Splitting UBU (SMS-UBU)

Initialize $(x_0, v_0) \in \mathbb{R}^{2d}$, stepsize $h > 0$, friction parameter $\gamma > 0$ and number of minibatches N_m .
for $i = 1, 2, \dots, \lceil K/2N_m \rceil$ **do**
Sample $\omega_1, \dots, \omega_{N_m} \in [N_D]^{N_b}$ uniformly without replacement.

Forward Sweep

for $k = 1, 2, \dots, \min\{N_m, K - (2i - 2)N_m\}$ **do**

Sample $Z_k^x, Z_k^v, \tilde{Z}_k^x, \tilde{Z}_k^v$ according to (2.8)

(U) $(x, v) \rightarrow (x_{(2i-2)N_m+k-1} + \frac{1-\eta^{1/2}}{\gamma}v_{(2i-2)N_m+k-1} + Z_k^x, \eta^{1/2}v_{(2i-2)N_m+k-1} + Z_k^v)$

(B) $v \rightarrow v - h\mathcal{G}(x, \omega_k)$

(U) $(x_{2N_m i+k}, v_{2N_m i+k}) \rightarrow (x + \frac{1-\eta^{1/2}}{\gamma}v + \tilde{Z}_k^x, \eta^{1/2}v + \tilde{Z}_k^v)$

end for

Backward Sweep

for $k = 1, 2, \dots, \min\{N_m, K - (2i - 1)N_m\}$ **do**

Sample $Z_k^x, Z_k^v, \tilde{Z}_k^x, \tilde{Z}_k^v$ according to (2.8)

(U) $(x, v) \rightarrow (x_{(2i-1)N_m+k-1} + \frac{1-\eta^{1/2}}{\gamma}v_{(2i-1)N_m+k-1} + Z_k^x, \eta^{1/2}v_{(2i-1)N_m+k-1} + Z_k^v)$

(B) $v \rightarrow v - h\mathcal{G}(x, \omega_{N_m+1-k})$

(U) $(x_{(2i-1)N_m+k}, v_{(2i-1)N_m+k}) \rightarrow (x + \frac{1-\eta^{1/2}}{\gamma}v + \tilde{Z}_k^x, \eta^{1/2}v + \tilde{Z}_k^v)$

end for

end for

Output: Samples $(x_k)_{k=0}^K$.

3 Theory

In this section we present theoretical results related to SMS-UBU. We provide the key assumptions to establish a Wasserstein contraction result related to the convergence of our numerical scheme, and we give a global error estimate which establishes the $\mathcal{O}(h^2)$ strong accuracy bound, where h is the stepsize used. Proofs of these results are deferred to the appendix.

3.1 Assumptions

We first state the assumptions used in our proofs.

Assumption 3. f is m -strongly convex if there exists a $m > 0$ such that for all $x, y \in \mathbb{R}^d$

$$\langle \nabla f(x) - \nabla f(y), x - y \rangle \geq m \|x - y\|^2.$$

Assumption 4. $f : \mathbb{R}^d \rightarrow \mathbb{R}$ is C^2 , and there exists $M > 0$ such that for all $x, y \in \mathbb{R}^d$

$$\|\nabla f(x) - \nabla f(y)\| \leq M \|x - y\|.$$

Assumption 5. The potential $f : \mathbb{R}^d \rightarrow \mathbb{R}$ is C^3 and there exists $M_1 > 0$ such that for all $x, y \in \mathbb{R}^d$,

$$\|\nabla^2 f(x) - \nabla^2 f(y)\| \leq M_1 \|x - y\|,$$

this implies that

$$\|\nabla^3 f(x)[v, v']\| \leq M_1 \|v\| \|v'\|,$$

as used in [51].

The strongly Hessian Lipschitz property relies on a specific tensor norm from [15], which we use to establish improved dimension dependence. A small strongly Hessian Lipschitz constant for $\nabla^3 f$ is shown to hold in specific applications of practical interest (see [15] and [10]).

Definition 2. For $A \in \mathbb{R}^{d \times d \times d}$, let

$$\|A\|_{\{1,2\}\{3\}} = \sup_{x \in \mathbb{R}^{d \times d}, y \in \mathbb{R}^d} \left\{ \sum_{i,j,k=1}^d A_{ijk} x_{ij} y_k \left| \sum_{i,j=1}^d x_{ij}^2 \leq 1, \sum_{k=1}^d y_k^2 \leq 1 \right. \right\}.$$

Remark 2. The $\|A\|_{\{1,2\}\{3\}}$ norm in Definition 2 can be equivalently written as

$$\|A\|_{\{12\}\{3\}} = \left\| \sum_{i_1} A_{i_1, \cdot, \cdot}^T \cdot A_{i_1, \cdot, \cdot} \right\|^{1/2}, \quad (3.1)$$

where $\|\cdot\|$ refers to the L^2 matrix norm, and $A_{i_1, \cdot, \cdot} = (A_{i_1, i_2, i_3})_{1 \leq i_2 \leq d, 1 \leq i_3 \leq d}$ is a $d \times d$ matrix, see the proof of Lemma 7 of [48].

Assumption 6 (M_1^s -strongly Hessian Lipschitz). $f : \mathbb{R}^d \rightarrow \mathbb{R}$ is three times continuously differentiable and M_1^s -strongly Hessian Lipschitz if there exists $M_1^s > 0$ such that

$$\|\nabla^3 f(x)\|_{\{1,2\}\{3\}} \leq M_1^s,$$

for all $x \in \mathbb{R}^d$.

3.2 Convergence of the numerical method

In this subsection, we summarize Wasserstein convergence results from [10] which used the technique developed in [38]. There have been many works on couplings of kinetic Langevin dynamics and its discretization including [16], [21], [43], [51], [11], [53] in the discretized setting and [23], [52] in the continuous setting. We remark that Wasserstein convergence for the UBU discretization was first studied in [51].

Definition 3 (Weighted Euclidean norm). For $z = (x, v) \in \mathbb{R}^{2d}$ the weighted Euclidean norm of z is defined by

$$\|z\|_{a,b}^2 = \|x\|^2 + 2b \langle x, v \rangle + a \|v\|^2,$$

for $a, b > 0$ with $b^2 < a$.

Remark 3. Using the assumption $b^2 < a$, we can show that this is equivalent to the Euclidean norm on \mathbb{R}^{2d} . Under the condition $b^2 \leq a/4$, we have

$$\frac{1}{2} \min(a, 1) \|z\|^2 \leq \frac{1}{2} \|z\|_{a,0}^2 \leq \|z\|_{a,b}^2 \leq \frac{3}{2} \|z\|_{a,0}^2 \leq \frac{3}{2} \max(a, 1) \|z\|^2. \quad (3.2)$$

Definition 4 (p -Wasserstein distance). Let us define $\mathcal{P}_p(\mathbb{R}^{2d})$ to be the set of probability measures which have p -th moment for $p \in [1, \infty)$ (i.e. $\mathbb{E}(\|Z\|^p) < \infty$). Then the p -Wasserstein distance in norm $\|\cdot\|_{a,b}$ between two measures $\mu, \nu \in \mathcal{P}_p(\mathbb{R}^{2d})$ is defined as

$$\mathcal{W}_{p,a,b}(\nu, \mu) = \left(\inf_{\xi \in \Gamma(\nu, \mu)} \int_{\mathbb{R}^{2d}} \|z_1 - z_2\|_{a,b}^p d\xi(z_1, z_2) \right)^{1/p}, \quad (3.3)$$

where $\|\cdot\|_{a,b}$ is the norm introduced before and that $\Gamma(\nu, \mu)$ is the set of measures with respective marginals of ν and μ .

Remark 4. We use \mathcal{W}_2 to mean the standard Wasserstein-2 distance (equivalent to $\mathcal{W}_{2,1,0}$).

Proposition 5 (Proposition C.6 of [10]). Suppose that f satisfies Assumptions 3 and 4. Let $a = \frac{1}{M}$, $b = \frac{1}{\gamma}$, $c(h) = \frac{mh}{8\gamma}$ and P_h denote the transition kernel for a step of UBU with stepsize h . For all $\gamma \geq \sqrt{8M}$, $h < \frac{1}{2\gamma}$, $1 \leq p \leq \infty$, $\mu, \nu \in \mathcal{P}_p(\mathbb{R}^{2d})$ and for all $n \in \mathbb{N}$,

$$\mathcal{W}_{p,a,b}(\nu P_h^n, \mu P_h^n) \leq (1 - c(h))^n \mathcal{W}_{p,a,b}(\nu, \mu).$$

Further to this, P_h has a unique invariant measure π_h satisfying that $\pi_h \in \mathcal{P}_p(\mathbb{R}^{2d})$ for all $1 \leq p \leq \infty$.

3.3 Error estimates

Theorem 6. Consider the SMS-UBU scheme with friction parameter $\gamma > 0$, stepsize $h > 0$ and initial measure π_0 and assume that $h < \frac{1}{2\gamma}$ and $\gamma \geq \sqrt{8M}$. Let the potential f be M - ∇ Lipschitz and of the form $f = \sum_{i=1}^{N_m} f_i$, where each f_i is m_i -strongly convex for $i = 1, \dots, N_m$ and M/N_m - ∇ Lipschitz with minimizer $x^* \in \mathbb{R}^d$. Consider the measure of the position k -th SMS-UBU, denoted by $\tilde{\pi}_k$, which approximates the target measure π for a potential f that is M_1 -Hessian Lipschitz. We have that

$$\mathcal{W}_2(\tilde{\pi}_k, \pi) \leq \sqrt{2} \exp\left(-\frac{mh}{8\gamma} \left\lfloor \frac{k}{N_m} \right\rfloor\right) \mathcal{W}_{2,a,b}(\pi_0, \bar{\pi}) + C(\gamma, m, M, M_1, N_m) h^2 d,$$

and if f is M_1^s -strongly Hessian Lipschitz we have that

$$\mathcal{W}_2(\tilde{\pi}_k, \pi) \leq \sqrt{2} \exp\left(-\frac{mh}{8\gamma} \left\lfloor \frac{k}{N_m} \right\rfloor\right) \mathcal{W}_{2,a,b}(\pi_0, \bar{\pi}) + C(\gamma, m, M, M_1^s, N_m) h^2 \sqrt{d}.$$

If we impose the stronger stepsize restriction $h < 1/(12\gamma N_m)$, then our bounds simplify to the form

$$\mathcal{W}_2(\tilde{\pi}_k, \pi) \leq \sqrt{2} \exp\left(-\frac{mh}{8\gamma} \left\lfloor \frac{k}{N_m} \right\rfloor\right) \mathcal{W}_{2,a,b}(\pi_0, \bar{\pi}) + C(\tilde{\gamma}, \tilde{m}, \tilde{M}, \tilde{M}_1^s) h^2 N_m^{5/2} \sqrt{d},$$

where $\tilde{\gamma} = \gamma/\sqrt{N_m}$, $\tilde{m} = m/N_m$, $\tilde{M} = M/N_m$ and $\tilde{M}_1^s = M_1^s/N_m$, and similarly when we don't assume the potential is strongly Hessian Lipschitz.

Proof. For $k \in \mathbb{N}$ define (\hat{x}_k, \hat{v}_k) to be SMS-UBU and $(X_t, V_t)_{t \geq 0}$ to be (2.1), both initialized at the target measure $(\hat{x}_0, \hat{v}_0) := (X_0, V_0) \sim \bar{\pi}$ then,

$$\begin{aligned} \|x_k - X_{kh}\|_{L^2} &\leq \|x_k - \hat{x}_k\|_{L^2} + \|\hat{x}_k - X_{kh}\|_{L^2} \\ &\leq \sqrt{2} \|(x_k - \hat{x}_k, v_k - \hat{v}_k)\|_{L^2, a, b} + \|\hat{x}_k - X_{kh}\|_{L^2} \\ &\leq \sqrt{2} \exp\left(-\frac{mh}{8\gamma} \left\lfloor \frac{k}{N_m} \right\rfloor\right) \|(x_0 - X_0, v_0 - V_0)\|_{L^2, a, b} + \|\hat{x}_k - X_{kh}\|_{L^2}, \end{aligned}$$

where the final term can be bounded by Theorem 12 under appropriate assumptions. \square

Theorem 7. Considering the SMS-UBU scheme with friction parameter $\gamma > 0$, stepsize $h > 0$, initial measure π_0 and assuming that $h < \frac{1}{2\gamma}$, $\gamma \geq \sqrt{8M}$ and the stochastic gradient satisfies Assumptions 2 with constants C_{SG} . Let the potential f be M - ∇ Lipschitz, m -strongly convex and of the form $f = \sum_{i=1}^{N_m} f_i$, where each f_i is m_i -strongly convex, where $m = \sum_{i=1}^{N_m} m_i$. Then at the k -th iteration, and its measure π^k we have the non-asymptotic bound

$$\begin{aligned} \mathcal{W}_{2,a,b}(\pi^k, \bar{\pi}) &\leq \exp\left(-\frac{mh}{8\gamma} \left\lfloor \frac{k}{N_m} \right\rfloor\right) \mathcal{W}_{2,a,b}(\pi_0, \bar{\pi}) \\ &\quad + C(\gamma/\sqrt{N_m}, m/N_m, M/N_m) \left[\frac{C_{SG} \sqrt{h}}{N_m^{1/4}} + h \right] \sqrt{d}. \end{aligned}$$

Remark 5. When using random permutations we have an unbiased estimator of the force at each step and we can achieve similar bounds as [27] and [20] which allows us to improve upon our bounds in the large N_m , and large stepsize setting. This is the result of Theorem 7. We remark we prove a corresponding result in the simpler setting with vanilla stochastic gradients for UBU (see Theorem 13).

Remark 6. These results can be extended to the non-convex setting using the results of [52] or [53] under appropriate assumptions (convexity outside a ball), using contraction results of the continuous or discrete dynamics. The dimension and stepsize dependence would be as in the convex case, with additional dependence on the radius of the ball of non-convexity.

3.4 Bias of integrators for multinomial regression

To illustrate the $O(h^2)$ bias for SMS-UBU, we have conducted an experiment in Bayesian multinomial logistic regression ([7]) on the Fashion-MNIST dataset ([60]). We have used a isotropic Gaussian prior (quadratic regularizer) of the form $p(x)dx \propto \exp(-\|x\|^2/(2\sigma^2))dx$ with $\sigma = 50^{-1/2}$. The potential is strongly convex and log-concave. Using the L-BFGS algorithm, we found the global minimizer x^* , and initiated sampling algorithms from this. We have considered 5 sampling algorithms: SG-HMC based on Euler-Mayurama discretization of kinetic Langevin ([13]), as well as SG-BAOAB, SMS-BAOAB, SG-UBU, and SMS-UBU. Batch sizes were chosen as 200 (out of training size 60000), and we have implemented variance reduction (2.7) with respect to x^* . As test functions, we have used the posterior probabilities on the correct class on the test dataset (10000 images, so 10000 probabilities). Our bias estimates are shown on Figure 3.4.

To evaluate the bias accurately, we have constructed synchronous couplings of chains at stepsizes h and $h/2$, by making them share the same Brownian noise (for example, if the SG-HMC chain in Algorithm 5 at stepsize $h/2$ uses Gaussians ξ_{2k-1} and ξ_{2k} at steps $2k-1$ and $2k$, then the coupled chain at stepsize h uses $(\xi_{2k-1} + \xi_{2k})/\sqrt{2}$ at step k). Such couplings allowed us to estimate biases more accurately as the variance of the differences becomes significantly smaller compared to using independent chains, while the expected value of the differences remains the same. The maximum stepsize below which stability issues occurred was $h_0 = 2 \cdot 10^{-3}$. Let $h_l = h_0 \cdot 2^{-l}$ for $l \geq 0$. We have constructed couplings between chains with stepsizes $(h_0, h_1), (h_1, h_2), \dots, (h_5, h_6)$, run coupled chains for $400 \cdot 2^l$ epochs for levels (h_l, h_{l+1}) , discarded 20% of the samples as burn-in, and used the rest for estimating the difference in expectations between stepsizes h_l and h_{l+1} . We have estimated the full bias using the telescoping sum $\pi_{h_0}(g) - \pi_{h_6}(g) = (\pi_{h_0}(g) - \pi_{h_1}(g)) + \dots + (\pi_{h_5}(g) - \pi_{h_6}(g))$, assuming that the bias π_{h_6} is negligible. We have estimated the standard deviation of these bias estimates by breaking the total simulation run into 4 chunks of equal size, computing bias estimates based on each one separately, and then computing the standard deviations.

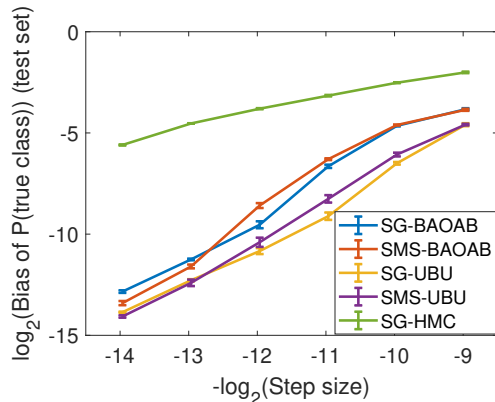


Figure 1: Average bias of probability of true class on test dataset for five integrators as a function of stepsize.

In addition to evaluating the biases, we have also performed further calibration checks in terms of acceptance rate of the posterior mean estimators of predictive probabilities of each class, as well as average negative log-likelihood on test set (NLL), adaptive calibration error (ACE) [46], as well as Ranked Probability Score (RPS) [18] (which is equivalent to the Brier score when there are 2 classes). Standard deviations for these quantities were also computed in the same way as for the biases. As Figure 2 shows, SMS-UBU outperforms the alternative methods in terms of calibration performance, and accuracy at the largest stepsizes, and it has a significantly smaller bias compared to BAOAB and Euler-Mayurama integrators. Our plots are well aligned with the theoretical results showing $O(\sqrt{d}h^2)$, and the dimension dependency seems even better for these test functions, in line with the results in [14].

In [17], a symmetric minibatch splitting version of HMC was proposed, including a Metropolis-

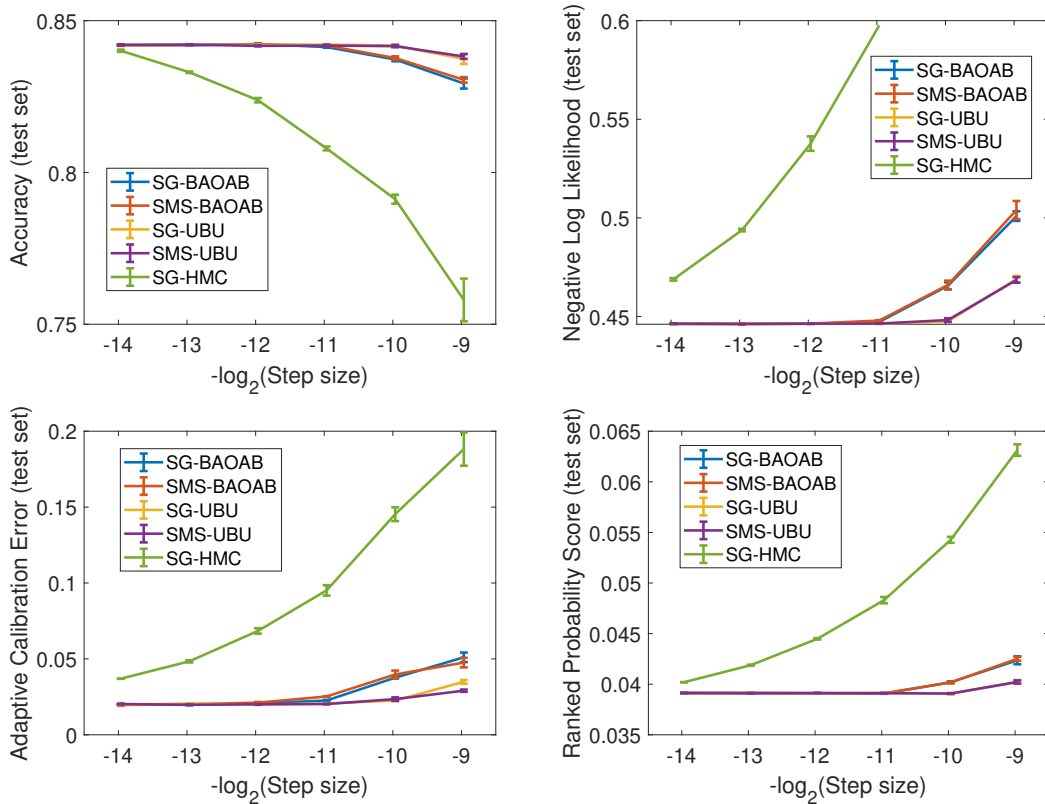


Figure 2: The effect of stepsize on accuracy and calibration performance (NLL, ACE, and RPS).

Hastings accept/reject step. As a comparison, we have implemented Metropolis method this for the same multinomial logistic regression example, using the same variance reduction scheme on the potentials, using the same batch size and dataset. We have also tried a slightly modified version of the scheme of [17], stated in Algorithm 3. This version is different from the original scheme in terms of the type of leapfrog steps used (first a half step in position update, followed by a full step in velocity update, and then another half step in position update), and the partial velocity refreshment step (as in Generalized HMC [28]). At the same step sizes, we found that Algorithm 3 had significantly higher acceptance rates compared to the original scheme in [17]. We did some tuning of the parameters, and obtained the best performance $h = 10^{-5}$, $L = 10$, and $\alpha = 0.7$. With $K = 1000$ iterations, the acceptance rate was 0.844. We discarded 20% of the samples as burn-in, and computed the calibration performance based on the remaining ones. Accuracy was 0.8420, ACE was 0.0195, NLL was 0.4464, and RPS was 0.0391.

Comparing with Figure 2, we can see that the calibration results are essentially the same as for SMS-UBU and the other unadjusted methods, confirming that both have very low bias. Nevertheless, the step size $h = 10^{-5}$ ($\log_2 h \approx -16.61$) for SMS-GHMC is 100 times smaller than the step size $h = 10^{-3}$ at which SMS-UBU was already offering essentially the same calibration performance. Hence the Metropolized method SMS-GHMC is much more computationally expensive in this example compared to the unadjusted ones based on second-order integrators.

Algorithm 3 Symmetric Minibatch Splitting Generalized HMC (SMS-GHMC)

Initialize $(x_0, v_0) \in \mathbb{R}^{2d}$, stepsize $h > 0$, number of minibatches N_m , number of sweeps per accept/reject step L , partial refreshment parameter $\alpha \in [0, 1)$, number of iterations K .

for $k = 1, 2, \dots, K$ **do**

Sample $\omega_1, \dots, \omega_{N_m} \in [N_D]^{N_b}$ uniformly without replacement

$(x, v) \rightarrow (x_{k-1}, v_{k-1})$

for $l = 1, 2, \dots, L$ **do**

Forward Sweep

for $b = 1, 2, \dots, N_m$ **do**

$x \rightarrow x + \frac{h}{2}v$

$v \rightarrow v - h\mathcal{G}(x, \omega_b)$

$x \rightarrow x + \frac{h}{2}v$

end for

Backward Sweep

for $b = 1, 2, \dots, N_m$ **do**

$x \rightarrow x + \frac{h}{2}v$

$v \rightarrow v - h\mathcal{G}(x, \omega_{N_m+1-b})$

$x \rightarrow x + \frac{h}{2}v$

end for

end for

Metropolis-Hastings Accept/Reject Step

Compute difference of Hamiltonians $H(x_{k-1}, v_{k-1}) - H(x, v) = f(x_{k-1}) + \frac{\|v_{k-1}\|^2}{2} - f(x) - \frac{\|v\|^2}{2}$.

Sample $U_k \sim \text{Uniform}[0, 1]$.

if $\log(U_k) < H(x_{k-1}, v_{k-1}) - H(x, v)$ **then**

$(x_k, v_k) = (x, v)$

else

$(x_k, v_k) = (x_{k-1}, -v_{k-1})$.

end if

Velocity Refreshment Step

Sample $Z_k \sim \mathcal{N}(0_d, I_d)$

Update $v_k \rightarrow \alpha v_k + \sqrt{1 - \alpha^2}Z_k$

end for

Output: Samples $(x_k)_{k=0}^K$.

4 Bayesian uncertainty quantification in neural networks via sampling

In this section, we explain the use of our sampling methods for exploring the posterior distributions of the parameters of neural networks. The theory is based on a unimodality assumption (log-concave target distribution) whose potential has a bounded second derivative. It is well known that the loss functions of neural networks are highly multimodal and can have minimizers in areas of high curvature, i.e. the norm of the Hessian may be large. Sampling from such multimodal distributions is highly challenging, and mixing can be slow even if full gradients are used ([30]).

There has been a significant amount of effort in the literature to find minimizers that lie in flat regions with low curvature, see ([4], [24]). In the experiments of this paper, we have used a slowly decreasing stepsize combined with Stochastic Weight Averaging (SWA) ([29]) to find flat minimizers. We can assess the flatness of an area near a point via the norm of the Hessian of the log-posterior at the point, which can be efficiently computed using the power iteration method ([42]). Figure 3 shows the typical norm of the Hessian of log-posterior for a CNN-based neural network trained for classification on the Fashion-MNIST dataset.

As we can see, the Hessian has a norm of up to 3×10^7 for a network with random weights, but it has much smaller norm near local minimizers, and especially at the SWA points. Adding some Gaussian noise to the SWA network leads to a significant increase in the norm of the Hessian, but remains small compared to using random weights. This observation, together with our theoretical understanding of convergence properties of kinetic Langevin dynamics integrators, leads us to focus on exploring the relatively smooth area in the neighbourhood of the SWA network optima.

Algorithm 4 Ensemble SMS-UBU with SWA centred local approximation

Input: Stepsize $h > 0$, friction parameter $\gamma > 0$. Number of sampling steps K , number of training epochs T_{train} , number of SWA epochs T_{SWA} . Localization parameters ρ, ρ_{max} .

for $n = 1, 2, \dots, N$ **do**

1. Randomly initialize the network weights.
2. Train network for T_{train} epochs at decreasing stepsize.
3. Continue training network with a fixed stepsize for T_{SWA} epochs, and accumulate the average weights over this period in variable $x_{(n)}^*$.
4. Obtain K samples from the distribution $\pi_{(n)}^*(x) \propto \exp\left(-f(x) - \frac{\|x - x_{(n)}^*\|^2}{2\rho^2}\right)$ using SMS-UBU initiated at $x_0 = x_{(n)}^*$, $v_0 \sim N(0, I_d)$, with elastic bounces when exiting hypercube $\Omega_{(n)} = \{x : \|x - x_{(n)}^*\|_\infty < \rho_{\text{max}}\}$.

end for

Output: Samples $(x_k^{(n)})_{k \in 1:K, n \in 1:N}$.

Let x^* the SWA weights found by the algorithm. Instead of exploring the multimodal target $\pi(dx) \propto \exp(-f(x))dx$, we propose the localized distribution $\pi^*(x)$ and potential energy $f^*(x)$ defined by

$$\pi^*(dx) \propto \exp(-f^*(x))dx \text{ for } \|x - x^*\|_\infty < \rho_{\text{max}}, \quad f^*(x) = f(x) + \frac{1}{2\rho^2}\|x - x^*\|^2,$$

where $\rho, \rho_{\text{max}} > 0$ are so-called localization parameters. $f^*(x)$ will be strongly convex due to inclusion of the quadratic regularizer term $\frac{1}{2\rho^2}\|x - x^*\|^2$ (for sufficiently small ρ). We further restrict the parameters to the hypercube $\Omega = \{x : \|x - x^*\|_\infty < \rho_{\text{max}}\}$ which ensures that the norm of the Hessian $\|\nabla^2(f^*(x))\|$ is relatively small within the domain Ω (see Figure 3). Although our Algorithm 2 was stated for an unconstrained domain, it is straightforward to adapt it to the hypercube Ω by implementing elastic bounces independently in each component whenever the x component exits the domain (recent theoretical results for numerical integrators on constrained spaces suggest that such bounces do not change the order of accuracy, see [34]). We chose $\rho_\infty = 6\rho$ in our experiments, which ensured that bounces rarely happened. Figure 4 shows the average training loss function for 4 independent SMS-UBU paths over 40 epochs started from x^* plus a multivariate Gaussian with standard deviation $\rho = 50^{-1/2}$. We have repeated this experiment 16 times, and plotted the \hat{R} values (Gelman-Rubin diagnostics, computed after 10 epochs of burn-in). Both of these plots indicate that SMS-UBU is able to approximate the localized distribution π^* efficiently. The good mixing properties for exploring π^* are dramatically better compared to earlier experiments that try to explore the whole target π ([30]), and the additional computational cost for this sampling (40 epochs) is only twice as much as the original training (20 epochs).

The local approximation π^* can still be far away from the original multimodal distribution π . To obtain a better approximation, we can use ensembles of independently obtained SWA points x_1^*, \dots, x_N^* , and run N independent SMS-UBU chains initiated from these points. The full details of our approach are stated in Algorithm 4.

5 Experiments

In this section, we evaluate the accuracy and calibration performance of ensembles of deep Bayesian neural networks on three datasets: Fashion-MNIST ([60]), Celeb-A ([61]), and chest X-ray ([31]), see Table 1 for further information. The networks used had six convolutional layers combined with batch normalization and max pooling layers, followed by some Multilayer Perceptron layers (these were chosen as low-rank to reduce the memory without harming the performance). We have included the Pytorch code for these networks in Section C of the Appendix. In the Fashion-MNIST and Celeb-A examples, we did not use any data augmentation. For the chest X-ray experiments, we have used random rotations, shifts, cropping, and brightness changes to augment the dataset size to 47400, and then used those images for training. The basic setup in all experiments was the same: 15 epochs of initial training with a polynomially-decaying stepsize schedule with power

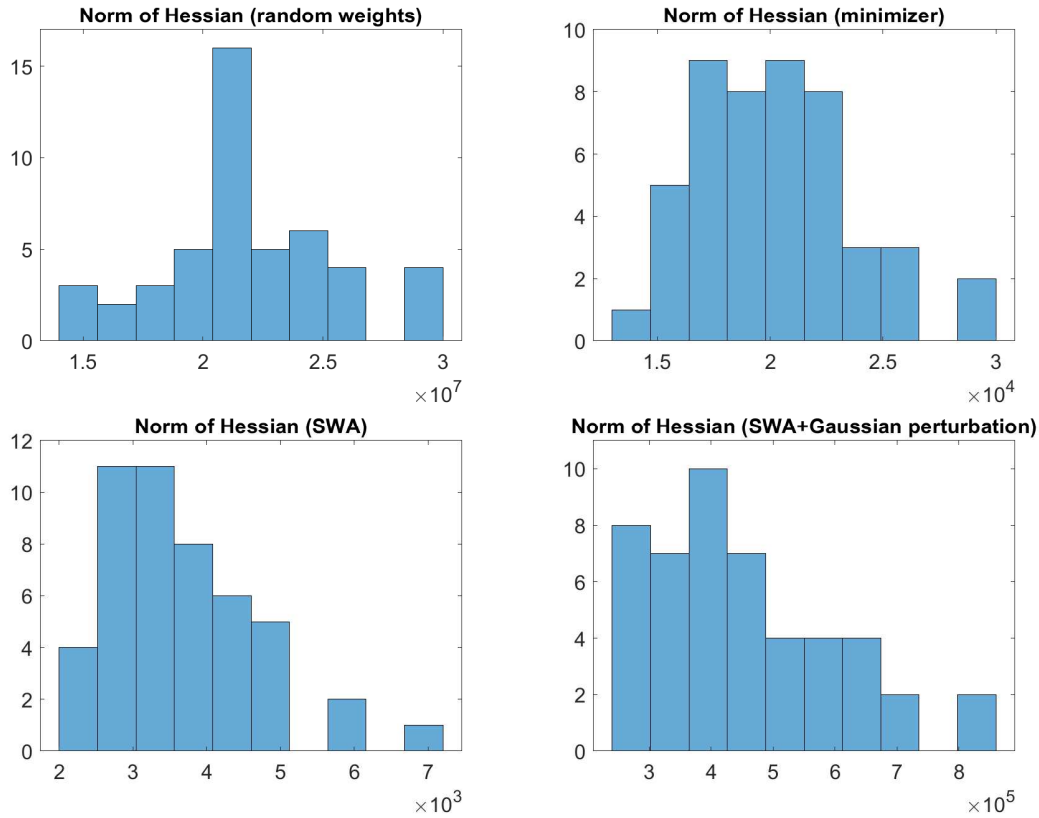


Figure 3: Norm of the Hessian for a CNN-based network for Fashion-MNIST at different points in the weight space over 48 independent runs: random initialisation, minimizer after 15 epochs of training (ADAM), Stochastic Weight Averaging over five epochs, and Gaussian perturbation of the SWA network

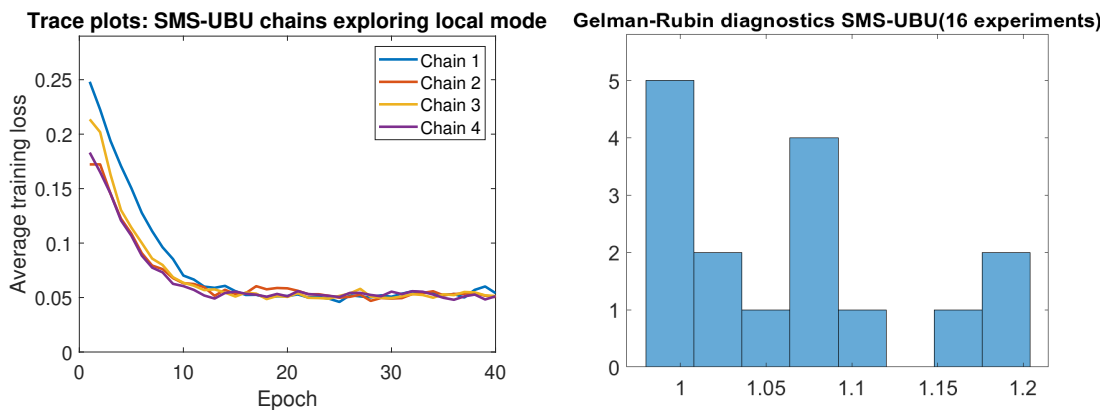


Figure 4: Left: trace plots for 4 SMS-UBU chains initialized at Gaussian perturbations of SWA weights. Right: Gelman-Rubin diagnostic \hat{R} of average training loss computed for 16 SWA weights x^* obtained independently (four parallel chains each). The four chains converge to the same level, and \hat{R} values are close to one, indicating excellent mixing.

Dataset	Training size	Test size	Resolution	Channels	# of param.
Fashion-MNIST	60000	10000	28×28	1	1265258
Celeb-A (blonde/brunette)	55400	6073	64×64	3	1612306
Chest X-ray	5217	600	180×180	1	870882

Table 1: Details about the datasets and neural networks used in our experiments

equal to one, followed by five epochs of stochastic weight averaging (SWA), and 40 epochs of SMS-UBU (ten epochs were discarded as burn-in, and the subsequent 30 epochs were then used as samples). Batch size was chosen as 200 in each case. In all datasets, quadratic regularisation with unit variance was applied on all weights but not the biases. An important implementation detail is that, to ensure a well-defined loss function, the batch normalization layers were not using running means, but only the current batch. To ensure good performance in the prediction task, we evaluated the network using a single larger batch consisting of 20 individual batches (4000 images) before predicting with network weights set to evaluation mode. In the Bayesian setting, no temperature parameter was used, but the potential was simply chosen as the total cross-entropy loss plus the regularizer. Our stepsize and other hyperparameter choices are stated in Table 2 of the Appendix.

We did 64 independent runs, and compared the performance of ensemble methods (ensembles after 15 epochs of training, ensembles of SWA networks, and ensembles of Bayesian samples according to Algorithm 4). The results are shown in figures 5, 6, and 7. Standard deviations for the tested quantities were computed based on the independent runs (for example, by pooling the runs into ensembles of size four, there were 16 independent such ensembles, etc.) As we can see, Bayesian networks can offer small gains in accuracy over ensembles of the same size, but more importantly, they can lead to significant gains in calibration performance (NLL, ACE, and RPS scores). The Bayesian approach provides a better modelling of uncertainty in the weights, which persists even with the local π^* used in Algorithm 4 (needed to improve conditioning for computational tractability).

6 Conclusion

We have proposed a new sampling algorithm for Bayesian neural network posteriors, based on a kinetic Langevin integrator combined with symmetric minibatching. We demonstrated a number of important results related to convergence of the numerical scheme, in terms of Wasserstein contraction, and also in terms of the derived estimates for weak error, establishing the accuracy to be $\mathcal{O}(h^2)$. Several numerical examples demonstrate the performance of SMS-UBU against other stochastic gradient schemes. A comparison was provided to both stochastic weight averaging and standard training (optimization). We obtained substantial improvements in calibration error. In terms of future work, one possibility are unbiased sampling methods for BNN posteriors (see [10] and [26]), which could provide an alternative to Metropolised methods such as [17].

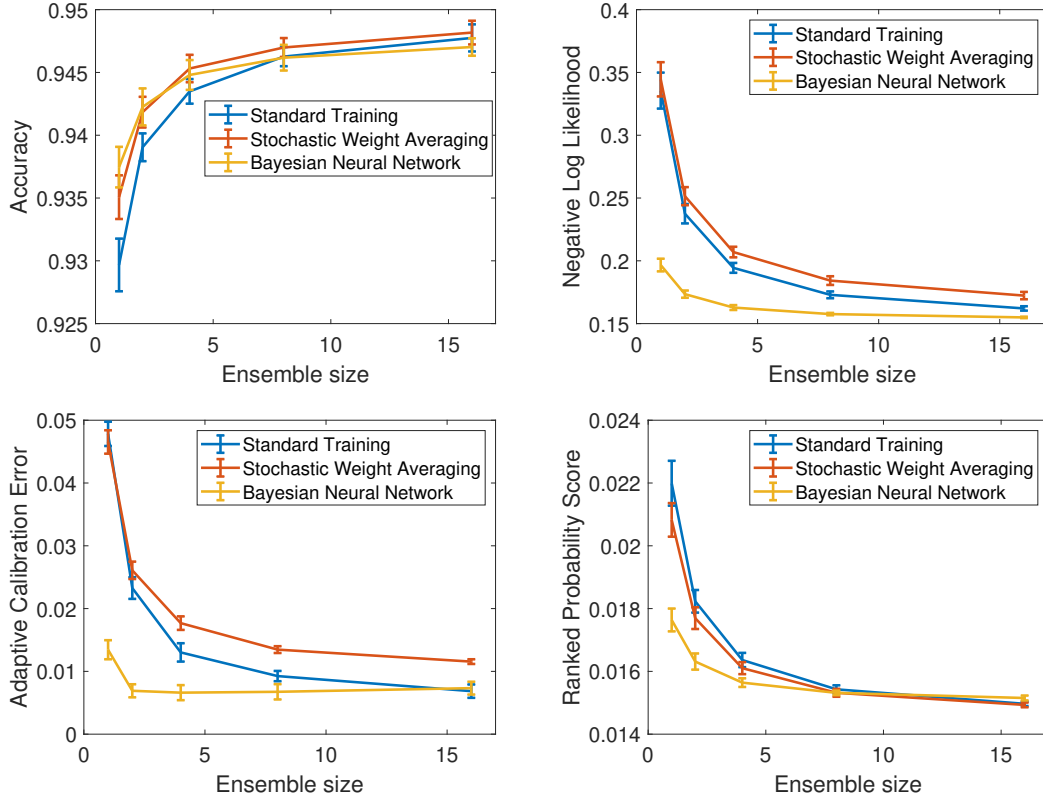


Figure 5: Accuracy and calibration results for a CNN-based network on Fashion-MNIST.

Appendix

A Algorithms

Algorithm 5 Stochastic Gradient Euler-Maruyama (SG-HMC)

- Initialize $(x_0, v_0) \in \mathbb{R}^{2d}$, stepsize $h > 0$ and friction parameter $\gamma > 0$.
 - for $k = 1, 2, \dots, K$ do
 - Sample $\omega_k \sim \rho$
 - Sample $\xi_k \sim \mathcal{N}(0_d, I_d)$
 - $x_k \rightarrow x_{k-1} + hv_{k-1}$
 - $v_k \rightarrow v_{k-1} - h\mathcal{G}(x_{k-1}, \omega_k) - h\gamma v_{k-1} + \sqrt{2\gamma h}\xi_k$
 - **Output:** Samples $(x_k)_{k=0}^K$.
-

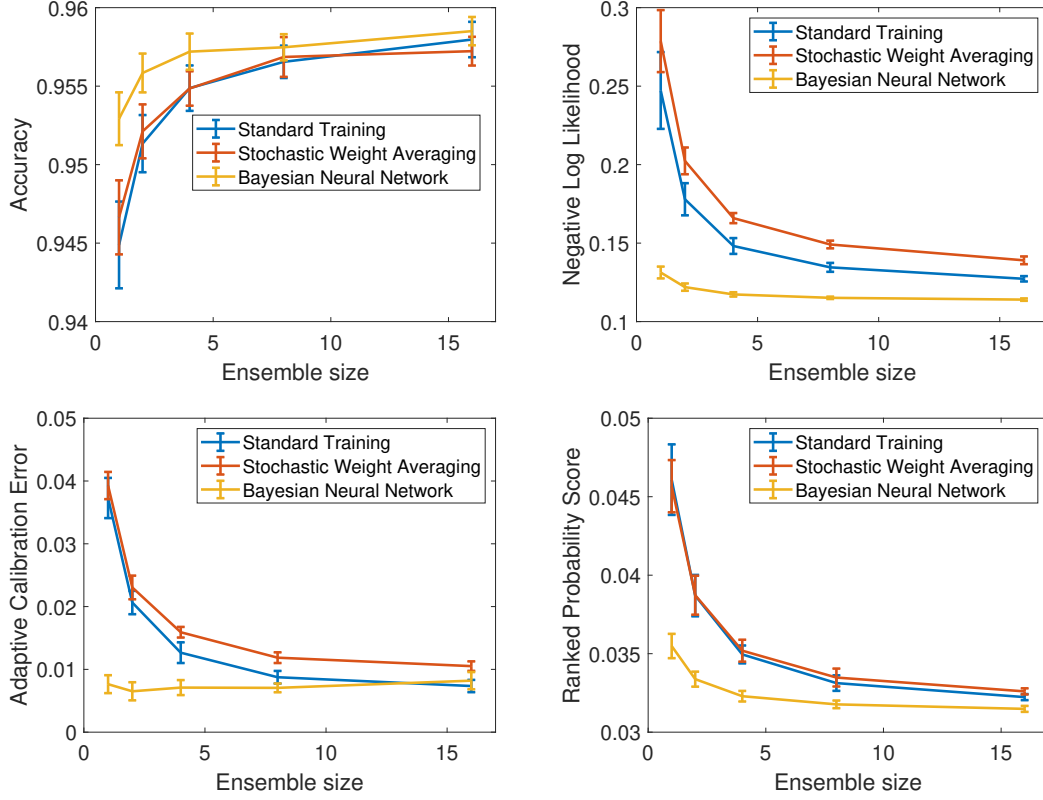


Figure 6: Accuracy and calibration results for a CNN-based network for classifying brown/blonde hair colour on the Celeb-A dataset.

Algorithm 6 Stochastic Gradient BAOAB (SG-BAOAB)

- Initialize $(x_0, v_0) \in \mathbb{R}^{2d}$, stepsize $h > 0$ and friction parameter $\gamma > 0$.
 - Sample $\omega_1 \sim \rho$
 - $G_0 \rightarrow \mathcal{G}(x_0, \omega_1)$
 - for $k = 1, 2, \dots, K$ do
 - (B) $v \rightarrow v_{k-1} - \frac{h}{2} G_{k-1}$
 - (A) $x \rightarrow x_{k-1} + \frac{h}{2} v$
Sample $\xi_k \sim \mathcal{N}(0_d, I_d)$
 - (O) $v \rightarrow \eta v + \sqrt{1 - \eta^2} \xi_k$
 - (A) $x_k \rightarrow x + \frac{h}{2} v$
Sample $\omega_{k+1} \sim \rho$
 $G_k \rightarrow \mathcal{G}(x_k, \omega_{k+1})$
 - (B) $v_k \rightarrow v - \frac{h}{2} G_k$
 - **Output:** Samples $(x_k)_{k=0}^K$.
-

B Proof of global strong order

We use the following formulation of kinetic Langevin dynamics in the analysis of the UBU scheme in the full gradient setting (as in [51]) and alternative schemes with the inexact gradient splitting methods.

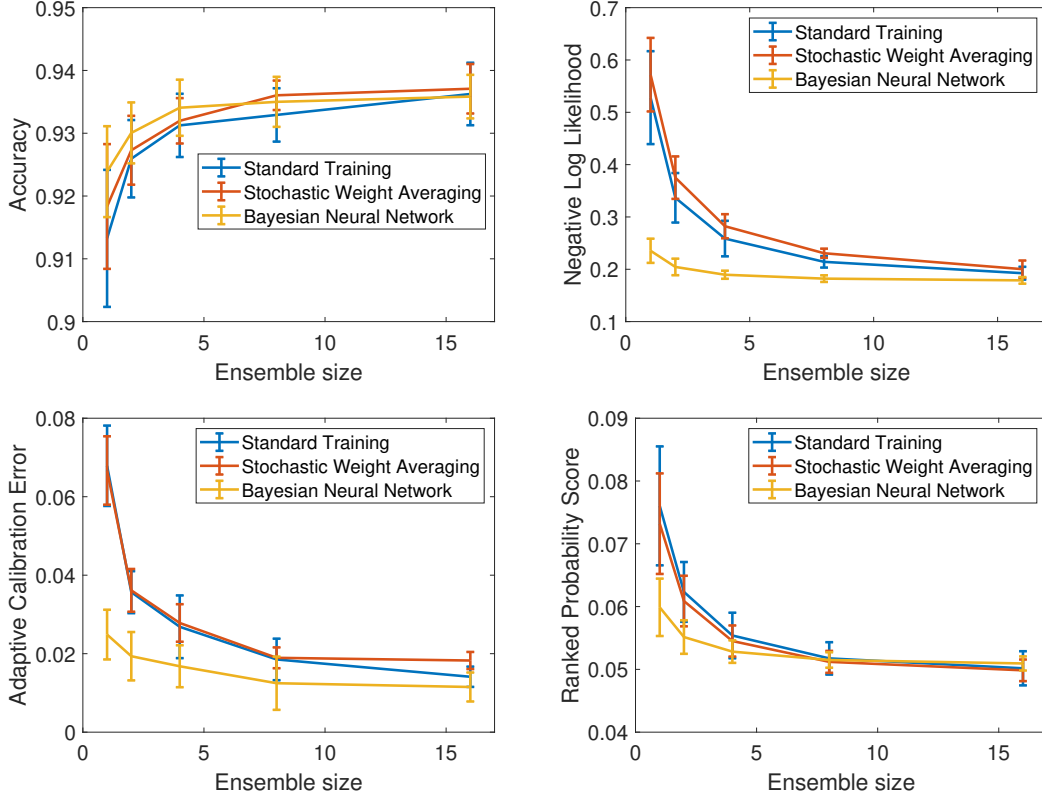


Figure 7: Accuracy and calibration results for a CNN-based network for detecting pneumonia on a chest X-ray dataset.

It is derived via Itô's formula on the product $e^{\gamma t}V_t$, we then have for initial condition $(X_0, V_0) \in \mathbb{R}^{2d}$:

$$V_t = \mathcal{E}(t)V_0 - \int_0^t \mathcal{E}(t-s)\nabla f(X_s)ds + \sqrt{2\gamma} \int_0^t \mathcal{E}(t-s)dW_s, \quad (\text{B.1})$$

$$X_t = X_0 + \mathcal{F}(t)V_0 - \int_0^t \mathcal{F}(t-s)\nabla f(X_s)ds + \sqrt{2\gamma} \int_0^t \mathcal{F}(t-s)dW_s, \quad (\text{B.2})$$

where

$$\mathcal{E}(t) = e^{-\gamma t} \quad \mathcal{F}(t) = \frac{1 - e^{-\gamma t}}{\gamma}. \quad (\text{B.3})$$

Then the UBU scheme (as in [51]) can be expressed as

$$v_{k+1} = \mathcal{E}(h)v_k - h\mathcal{E}(h/2)\nabla f(y_k) + \sqrt{2\gamma} \int_{kh}^{(k+1)h} \mathcal{E}((k+1)h-s)dW_s, \quad (\text{B.4})$$

$$y_k = x_k + \mathcal{F}(h/2)v_k + \sqrt{2\gamma} \int_{kh}^{(k+1/2)h} \mathcal{F}((k+1/2)h-s)dW_s, \quad (\text{B.5})$$

$$x_{k+1} = x_k + \mathcal{F}(h)v_k - h\mathcal{F}(h/2)\nabla f(y_k) + \sqrt{2\gamma} \int_{kh}^{(k+1)h} \mathcal{F}((k+1)h-s)dW_s, \quad (\text{B.6})$$

for comparison with the true dynamics via (B.1) and (B.2).

Algorithm 7 Symmetric Minibatch Splitting BAOAB (SMS-BAOAB)

Initialize $(x_0, v_0) \in \mathbb{R}^{2d}$, stepsize $h > 0$, friction parameter $\gamma > 0$ and number of minibatches N_m .

for $i = 1, 2, \dots, \lceil K/2N_m \rceil$ **do**

 Sample $\omega_1, \dots, \omega_{N_m} \in [N_D]^{N_b}$ uniformly without replacement.

 Define $\omega_{N_m+1} := \omega_1$.

if $i=1$ **then**

$G_0 \rightarrow \mathcal{G}(x_0, \omega_1)$.

else

$G_0 \rightarrow G_{N_m}$.

end if

Forward Sweep

for $k = 1, 2, \dots, \min\{N_m, K - (2i - 2)N_m\}$ **do**

 (B) $v \rightarrow v_{(2i-2)N_m+k-1} - \frac{h}{2}G_{k-1}$

 (A) $x \rightarrow x_{(2i-2)N_m+k-1} + \frac{h}{2}v$

 Sample $\xi_k \sim \mathcal{N}(0_d, I_d)$

 (O) $v \rightarrow \eta v + \sqrt{1 - \eta^2}\xi_k$

 (A) $x_{(2i-2)N_m+k} \rightarrow x + \frac{h}{2}v$

$G_k \rightarrow \mathcal{G}(x_k, \omega_{k+1})$

 (B) $v_{(2i-2)N_m+k} \rightarrow v - \frac{h}{2}G_k$

end for

Backward Sweep

for $k = 1, 2, \dots, \min\{N_m, K - (2i - 1)N_m\}$ **do**

 (B) $v \rightarrow v_{(2i-1)N_m+k-1} - \frac{h}{2}G_{N_m+1-k}$

 (A) $x \rightarrow x_{(2i-1)N_m+k-1} + \frac{h}{2}v$

 Sample $\xi_k \sim \mathcal{N}(0_d, I_d)$

 (O) $v \rightarrow \eta v + \sqrt{1 - \eta^2}\xi_k$

 (A) $x_{(2i-1)N_m+k} \rightarrow x + \frac{h}{2}v$

$G_k \rightarrow \mathcal{G}(x_k, \omega_{N_m+1-k})$

 (B) $v_{(2i-1)N_m+k} \rightarrow v - \frac{h}{2}G_k$

end for

end for

Output: Samples $(x_k)_{k=0}^K$.

We now define the stochastic gradient scheme (see Definition 1) by

$$\tilde{v}_{k+1} = \mathcal{E}(h)\tilde{v}_k - h\mathcal{E}(h/2)\mathcal{G}(\tilde{y}_k, \omega_{k+1}) + \sqrt{2\gamma} \int_{kh}^{(k+1)h} \mathcal{E}((k+1)h - s)dW_s, \quad (\text{B.7})$$

$$\tilde{y}_k = \tilde{x}_k + \mathcal{F}(h/2)\tilde{v}_k + \sqrt{2\gamma} \int_{kh}^{(k+1/2)h} \mathcal{F}((k+1/2)h - s)dW_s, \quad (\text{B.8})$$

$$\tilde{x}_{k+1} = \tilde{x}_k + \mathcal{F}(h)\tilde{v}_k - h\mathcal{F}(h/2)\mathcal{G}(\tilde{y}_k, \omega_{k+1}) + \sqrt{2\gamma} \int_{kh}^{(k+1)h} \mathcal{F}((k+1)h - s)dW_s. \quad (\text{B.9})$$

First considering the full gradient scheme we have the following L^2 error bound to the true diffusion.

Proposition 8. *Assume that $h < 1/2\gamma$ and $\gamma \geq \sqrt{M}$ and consider the kinetic Langevin dynamics and the UBU scheme (with full gradients and iterates $(x_n, v_n)_{n \in \mathbb{N}}$) with synchronously coupled Brownian motion initialized at the target measure $(\mathbf{X}_0, \mathbf{V}_0) = (X_0, V_0) \sim \pi$. Assume that Assumption 4 and Assumption 5 are satisfied, then for $k \in \mathbb{N}$ we have that for $(\Delta_x^k, \Delta_v^k) :=$*

$(x_k - X_{kh}, v_k - V_{kh})$

$$\|(\Delta_x^k, \Delta_v^k)\|_{L^2, a, b} \leq \frac{3\gamma^2}{M} e^{3 \max\{\gamma, \frac{2M}{\gamma}\} hk} \left(\mathbf{C} + \frac{5h^3}{48} (k+1) (5M + \gamma M^{1/2}) d^{1/2} \right),$$

where

$$\mathbf{C} = \gamma^{-1} (k+1) \frac{h^3 \sqrt{d}}{24} (3M_1 \sqrt{d} + M^{3/2} + \gamma M) + \sqrt{2\gamma^{-1}} \sqrt{\frac{(k+1)h^5 M^2 d}{192}},$$

and if Assumption 6 is satisfied this \mathbf{C} is refined to

$$\mathbf{C} = \gamma^{-1} (k+1) \frac{h^3 \sqrt{d}}{24} (3M_1^s + M^{3/2} + \gamma M) + \sqrt{2\gamma^{-1}} \sqrt{\frac{(k+1)h^5 M^2 d}{192}}.$$

Proof. Follows from exactly the same proof as [53, Lemma 13] with the choice of $\alpha = 5/2$ in L^2 rather than L^1 and the equivalence of norms. \square

Proposition 9. Suppose we have a SMS-UBU discretization with a potential which is M - ∇ Lipschitz and M_1 -Hessian Lipschitz and of the form $f = \sum_{i=1}^{N_m} f_i$, where $\nabla^2 f_i \prec MI_D/N_m$ for all $i = 1, \dots, N_m$, $h < \min\{\frac{1}{2\gamma}, \frac{1}{2\sqrt{M}}\}$, $l \in \mathbb{N}$ $(\tilde{\Delta}_x^{2lN_m}, \tilde{\Delta}_v^{2lN_m}) := (\tilde{x}_{2lN_m} - X_{2lN_m h}, \tilde{v}_{2lN_m} - V_{2lN_m h})$, where the discretization and continuous dynamics have synchronously coupled Brownian motion and they are all initialized at $(X_0, V_0) \sim \pi$, then

$$\|(\tilde{\Delta}_x^{2lN_m}, \tilde{\Delta}_v^{2lN_m})\|_{L^2, a, b} \leq e^{12hlN_m(h\gamma\sqrt{M}N_m + 3\sqrt{M})} (\mathbf{A}_1 + e^{6 \max\{\gamma, \frac{2M}{\gamma}\} hlN_m} \mathbf{A}_2),$$

where \mathbf{A}_1 and \mathbf{A}_2 are stated in the proof. If we assume that the potential further satisfies Assumption 6 then $M_1 d$, can simply be replaced by $M_1^s \sqrt{d}$ in \mathbf{A}_1 and \mathbf{A}_2 .

Remark 7. We could instead assume that $\nabla^2 f_i \prec M_i I_D$, for all $i = 1, \dots, N_m$, each f_i having a different gradient Lipschitz constant, but to simplify notation in the argument we assume the stronger assumption $\nabla^2 f_i \prec MI_D/N_m$.

Proof. We consider the position and velocity components separately.

Velocity component

Firstly, we write

$$\tilde{v}_{2N_m} - V_{2N_m h} = \underbrace{\tilde{v}_{2N_m} - v_{2N_m}}_{\text{(I)}} + \underbrace{v_{2N_m} - V_{2N_m h}}_{\text{(II)}}$$

and similarly, in x , we can bound the (II) using the full gradient scheme bounds in Proposition 8. Then we consider (I), the distance to full gradient discretization. We define $(\delta_x^k, \delta_v^k) := (\tilde{x}_k -$

$x_k, \tilde{v}_k - v_k$), for $k = 0, \dots, 2N_m$, then

$$\begin{aligned}
\delta_v^{2N_m} &= \mathcal{E}(h)\delta_v^{2N_m-1} - h\mathcal{E}(h/2)(N_m\nabla f_1(\tilde{y}_{2N_m-1}) - \nabla f(y_{2N_m-1})) \\
&= \mathcal{E}^{2N_m}(h)\delta_v^0 - h\mathcal{E}(h/2) \left[\sum_{i=0}^{N_m-1} \mathcal{E}(h)^{N_m-i} (N_m\nabla f_{N_m-i}(\tilde{y}_{N_m+i}) - \nabla f(y_{N_m+i})) \right. \\
&\quad \left. + \sum_{i=0}^{N_m-1} \mathcal{E}(h)^{i+N_m} (N_m\nabla f_{N_m-i}(\tilde{y}_{N_m-i-1}) - \nabla f(y_{N_m-i-1})) \right] \\
&= \mathcal{E}^{2N_m}(h)\delta_v^0 - h\mathcal{E}(h/2) \left[\sum_{i=0}^{N_m-1} \sum_{j=0}^{N_m-1} \mathcal{E}(h)^i (\nabla f_{N_m-i}(\tilde{y}_{N_m+i}) - \nabla f_{j+1}(y_{N_m+i})) \right. \\
&\quad \left. + \sum_{i=0}^{N_m-1} \sum_{j=0}^{N_m-1} \mathcal{E}(h)^{i+N_m} (\nabla f_{N_m-i}(\tilde{y}_{N_m-i-1}) - \nabla f_{j+1}(y_{N_m-i-1})) \right] \\
&= \mathcal{E}^{2N_m}(h)\delta_v^0 - h\mathcal{E}(h/2) \sum_{i=0}^{N_m-1} \mathcal{E}(h)^i \left[\sum_{j=0}^{N_m-1} (\nabla f_{N_m-i}(\tilde{y}_{N_m+i}) - \nabla f_{j+1}(y_{N_m+i})) \right. \\
&\quad \left. + \sum_{j=0}^{N_m-1} (\nabla f_{N_m-i}(\tilde{y}_{N_m-i-1}) - \nabla f_{j+1}(y_{N_m-i-1})) \right] \\
&\quad + h\mathcal{E}(h/2) (1 - \mathcal{E}(h)^{N_m}) \left[\sum_{i=0}^{N_m-1} \sum_{j=0}^{N_m-1} \nabla f_{N_m-i}(\tilde{y}_{N_m-i-1}) - \nabla f_{j+1}(y_{N_m-i-1}) \right] \\
&= \mathcal{E}^{2N_m}(h)\delta_v^0 + (\star) + (\dagger),
\end{aligned}$$

where without loss of generality we have assumed that they are ordered $1, \dots, N_D$ and allow for random permutations of this ordering.

Now we consider the two terms (\star) and (\dagger) in the last equality separately, as we have $1 - \mathcal{E}(h)^{N_m} \leq h\gamma N_m$, the second term is higher order in h .

More precisely,

$$\begin{aligned}
(\dagger) &= h\mathcal{E}(h/2) (1 - \mathcal{E}(h)^{N_m}) \left\| \sum_{i=0}^{N_m-1} \sum_{j=0}^{N_m-1} \nabla f_{N_m-i}(\tilde{y}_{N_m-i-1}) - \nabla f_{j+1}(y_{N_m-i-1}) \right\|_{L^2} \\
&\leq h^2\gamma M \sum_{i=0}^{N_m-1} \sum_{j=0}^{N_m-1} \|\tilde{y}_{N_m-i-1} - y_{N_m-j-1}\|_{L^2} \\
&\leq h^2\gamma M \sum_{i=0}^{N_m-1} \sum_{j=0}^{N_m-1} \left[\|\tilde{y}_{N_m-i-1} - X_{(N_m-i-1/2)h}\|_{L^2} \right. \\
&\quad \left. + \|X_{(N_m-i-1/2)h} - X_{(N_m-j-1/2)h}\|_{L^2} + \|X_{(N_m-j-1/2)h} - y_{N_m-j-1}\|_{L^2} \right] \\
&\leq h^2\gamma M \sum_{i=0}^{N_m-1} \sum_{j=0}^{N_m-1} \left[\|\Delta_x^{N_m-j-1}\|_{L^2} + h\|\Delta_v^{N_m-j-1}\|_{L^2} + \|\tilde{\Delta}_x^{N_m-i-1}\|_{L^2} \right. \\
&\quad \left. + h\|\tilde{\Delta}_v^{N_m-i-1}\|_{L^2} + 2h^2\sqrt{Md} + hN_m\sqrt{d} + h^2N_m^2\sqrt{Md} + \sqrt{2\gamma}(hN_m)^{3/2}\sqrt{d} \right].
\end{aligned}$$

We now consider the first term which is

$$\begin{aligned}
(\star) &= -h\mathcal{E}(h/2) \sum_{i=0}^{N_m-1} \mathcal{E}(h)^i \sum_{j=0}^{N_m-1} \left[C_{N_m-i}^i + \nabla f_{N_m-i}(\tilde{y}_{N_m+i}) - \nabla f_{N_m-i}(X_{(N_m+i+1/2)h}) \right. \\
&+ \nabla f_{N_m-i}(\tilde{y}_{N_m-i-1}) - \nabla f_{N_m-i}(X_{(N_m-i-1/2)h}) - C_{j+1}^i - \nabla f_{j+1}(y_{N_m+i}) + \nabla f_{j+1}(X_{(N_m+i+1/2)h}) \\
&\left. - \nabla f_{j+1}(y_{N_m-i-1}) + \nabla f_{j+1}(X_{(N_m-i-1/2)h}) \right],
\end{aligned}$$

where

$$C_i^j := \nabla f_i(X_{(N_m-j-1/2)h}) - 2\nabla f_i(X_{N_m h}) + \nabla f_i(X_{(N_m+j+1/2)h}),$$

for $i, j \in \{1, \dots, N_m\}$.

Considering the terms excluding the C_i^j , they can individually be bounded in L^2 by

$$\begin{aligned}
&hM \sum_{i=0}^{N_m-1} \left[\|\tilde{y}_{N_m+i} - X_{(N_m+i+1/2)h}\|_{L^2} + \|\tilde{y}_{N_m-i-1} - X_{(N_m-i-1/2)h}\|_{L^2} \right. \\
&\left. + \|y_{N_m+i} - X_{(N_m+i+1/2)h}\|_{L^2} + \|y_{N_m-i-1} - X_{(N_m-i-1/2)h}\|_{L^2} \right] \\
&\leq 2hM \sum_{i=0}^{N_m-1} \left[\left(\|\tilde{\Delta}_x^{N_m+i}\|_{L^2} + h\|\tilde{\Delta}_v^{N_m+i}\|_{L^2} + h^2\sqrt{Md} \right) \right. \\
&\left. + \left(\|\Delta_x^{N_m-i-1}\|_{L^2} + h\|\Delta_v^{N_m-i-1}\|_{L^2} + h^2\sqrt{Md} \right) \right].
\end{aligned}$$

Separately we can use Itô-Taylor expansion to bound the C_i^j as follows

$$\begin{aligned}
\nabla f_i(X_{N_m h}) &= \nabla f_i(X_{(N_m-j-1/2)h}) + (j+1/2)h\nabla^2 f_i(X_{(N_m-j-1/2)h})V_{(N_m-j-1/2)h} \\
&+ \int_0^{(j+1/2)h} \int_0^s d(\nabla^2 f_i(X_{s'+(N_m-j-1/2)h})V_{s'+(N_m-j-1/2)h})ds,
\end{aligned}$$

and applying Itô's formula as in [51] we have

$$\begin{aligned}
\nabla f_i(X_{N_m h}) &= \nabla f_i(X_{(N_m-j-1/2)h}) + (j+1/2)h\nabla^2 f_i(X_{(N_m-j-1/2)h})V_{(N_m-j-1/2)h} \\
&+ I_1^{i,j}(h) + I_2^{i,j}(h) + I_3^{i,j}(h) + I_4^{i,j}(h),
\end{aligned}$$

where

$$\begin{aligned}
I_1^{i,j}(h) &:= \int_0^{(j+1/2)h} \int_0^s \nabla^3 f_i(X_{s'+(N_m-j-1/2)h})[V_{s'+(N_m-j-1/2)h}, V_{s'+(N_m-j-1/2)h}]ds'ds \\
I_2^{i,j}(h) &:= -\gamma \int_0^{(j+1/2)h} \int_0^s \nabla^2 f_i(X_{s'+(N_m-j-1/2)h})V_{s'+(N_m-j-1/2)h}ds'ds \\
I_3^{i,j}(h) &:= -\int_0^{(j+1/2)h} \int_0^s \nabla^2 f_i(X_{s'+(N_m-j-1/2)h})\nabla f(X_{s'+(N_m-j-1/2)h})ds'ds \\
I_4^{i,j}(h) &:= \sqrt{2\gamma} \int_0^{(j+1/2)h} \int_0^s \nabla^2 f_i(X_{s'+(N_m-j-1/2)h})dB_{s'}ds.
\end{aligned}$$

Then

$$\nabla f_i(X_{(N_m-j-1/2)h}) - 2\nabla f_i(X_{N_m h}) + \nabla f_i(X_{(N_m+j+1/2)h}) = \sum_{k=1}^4 \left[I_k^{i,j}(2h) - 2I_k^{i,j}(h) \right],$$

and

$$\begin{aligned}\|I_1^{i,j}(h)\|_{L^2} &\leq 3N_m h^2 M_1 d/2, & \|I_2^{i,j}(h)\|_{L^2} &\leq N_m h^2 \gamma M \sqrt{d}/2, \\ \|I_3^{i,j}(h)\|_{L^2} &\leq N_m h^2 M \sqrt{M d}/2.\end{aligned}$$

We then need to be more careful with the $I_4^{i,j}(h)$ terms which are lower order in h individually, but we can use an independence property.

Combining all the previous estimates we have that

$$\begin{aligned}\delta_v^{2N_m} &= \mathcal{E}^{2N_m}(h)\delta_v^0 + (\dagger) \\ &+ \left[(\star) + h\mathcal{E}(h/2) \sum_{i=0}^{N_m-1} \mathcal{E}(h)^i \sum_{j=0}^{N_m-1} \left(I_4^{N_m-i,i}(2h) - 2I_4^{N_m-i,i}(h) - I_4^{j+1,i}(2h) + 2I_4^{j+1,i}(h) \right) \right] \\ &- h\mathcal{E}(h/2) \sum_{i=0}^{N_m-1} \mathcal{E}(h)^i \sum_{j=0}^{N_m-1} \left(I_4^{N_m-i,i}(2h) - 2I_4^{N_m-i,i}(h) - I_4^{j+1,i}(2h) + 2I_4^{j+1,i}(h) \right).\end{aligned}$$

Then after $2lN_m$ steps, where $l \in \mathbb{N}$, and is initialized at the target measure we have that

$$\begin{aligned}\|\delta_v^{2lN_m}\|_{L^2} &\leq h^2 \gamma M N_m \sum_{k=0}^{l-1} \sum_{i=0}^{N_m-1} \left[\|\Delta_x^{N_m+i+2kN_m}\|_{L^2} + h\|\Delta_v^{N_m+i+2kN_m}\|_{L^2} + \|\tilde{\Delta}_x^{N_m-i-1+2kN_m}\|_{L^2} \right. \\ &+ h\|\tilde{\Delta}_v^{N_m-i-1+2kN_m}\|_{L^2} + 2h^2\sqrt{Md} + hN_m\sqrt{d} + h^2N_m^2\sqrt{Md} + \sqrt{2\gamma}(hN_m)^{3/2}\sqrt{d} \left. \right] \\ &+ 2hM \sum_{k=0}^{l-1} \sum_{i=0}^{N_m-1} \left[\left(\|\tilde{\Delta}_x^{N_m+i+2kN_m}\|_{L^2} + h\|\tilde{\Delta}_v^{N_m+i+2kN_m}\|_{L^2} + h^2\sqrt{Md} \right) \right. \\ &+ \left. \left(\|\Delta_x^{N_m-i-1+2kN_m}\|_{L^2} + h\|\Delta_v^{N_m-i-1+2kN_m}\|_{L^2} + h^2\sqrt{Md} \right) \right] \\ &+ 6lh^3N_m^3 \left(3M_1d + \gamma M\sqrt{d} + M\sqrt{Md} \right) + 14(hN_m)^{5/2}\sqrt{2l\gamma dM} \\ &\leq (h^2\gamma M N_m + 2hM) \sum_{i=0}^{2lN_m-1} \left[\|\Delta_x^i\|_{L^2} + h\|\Delta_v^i\|_{L^2} + \|\tilde{\Delta}_x^i\|_{L^2} + h\|\tilde{\Delta}_v^i\|_{L^2} \right] \\ &+ lh^3\gamma M N_m^3 \left(7 + 2hN_m\sqrt{M} + \sqrt{2\gamma}(hN_m)^{1/2} \right) \sqrt{d} \\ &+ 18lh^3N_m^3 \left(M_1d + M\sqrt{Md} \right) + 14(hN_m)^{5/2}\sqrt{2l\gamma dM} \\ &\leq hC_1^V \sum_{i=0}^{2lN_m-1} \left[\|\Delta_x^i\|_{L^2} + h\|\Delta_v^i\|_{L^2} + \|\tilde{\Delta}_x^i\|_{L^2} + h\|\tilde{\Delta}_v^i\|_{L^2} \right] + lN_m h^3 C_2^V + \sqrt{lN_m} h^{5/2} C_3^V,\end{aligned}$$

where we have used that $\mathbb{E}[I_4^{i,j_1} I_4^{i,j_2}] = 0$ for $j_1 \neq j_2$.

Position component

Now considering the position we write

$$\tilde{x}_{2N_m} - X_{2N_m h} = \underbrace{\tilde{x}_{2N_m} - x_{2N_m}}_{(I)} + \underbrace{x_{2N_m} - X_{2N_m h}}_{(II)},$$

and we can bound the (II) using the full gradient scheme bounds in Proposition 8. Then we

consider (I), the distance to full gradient discretization and we have

$$\begin{aligned}
\delta_x^{2N_m} &= \delta_x^{2N_m-1} + \mathcal{F}(h)\delta_v^{2N_m-1} - h\mathcal{F}(h/2)(N_m\nabla f_1(\tilde{y}_{2N_m-1}) - \nabla f(y_{2N_m-1})) \\
&= \delta_x^0 + \mathcal{F}(h) \sum_{i=0}^{2N_m-1} \delta_v^i - h\mathcal{F}(h/2) \left[\sum_{i=0}^{N_m-1} (N_m\nabla f_{N_m-i}(\tilde{y}_{N_m+i}) - \nabla f(y_{N_m+i})) \right. \\
&\quad \left. + \sum_{i=0}^{N_m-1} (N_m\nabla f_{N_m-i}(\tilde{y}_{N_m-i-1}) - \nabla f(y_{N_m-i-1})) \right] \\
&= \delta_x^0 + \mathcal{F}(h) \sum_{i=0}^{2N_m-1} \delta_v^i - h\mathcal{F}(h/2) \left[\sum_{i=0}^{N_m-1} \sum_{j=0}^{N_m-1} (\nabla f_{N_m-i}(\tilde{y}_{N_m+i}) - \nabla f_{j+1}(y_{N_m+i})) \right. \\
&\quad \left. + \sum_{i=0}^{N_m-1} \sum_{j=0}^{N_m-1} (\nabla f_{N_m-i}(\tilde{y}_{N_m-i-1}) - \nabla f_{j+1}(y_{N_m-i-1})) \right],
\end{aligned}$$

and hence for $l \in \mathbb{N}$, by reordering the sum we have

$$\begin{aligned}
\|\delta_x^{2lN_m}\|_{L^2} &\leq h \sum_{i=0}^{2lN_m-1} \|\delta_v^i\|_{L^2} + \\
&h^2 \frac{M}{N_m} \left[\sum_{k=0}^{l-1} \sum_{i=0}^{N_m-1} \sum_{j=0}^{N_m-1} (\|\tilde{y}_{N_m+i+2kN_m} - y_{N_m+j+2kN_m}\|_{L^2} + \|\tilde{y}_{N_m-i-1+2kN_m} - y_{N_m-j-1+2kN_m}\|_{L^2}) \right] \\
&\leq h \sum_{i=0}^{2lN_m-1} \|\delta_v^i\|_{L^2} + h^2 M \left[\sum_{k=0}^{l-1} \sum_{i=0}^{N_m-1} \left(\|\tilde{\Delta}_x^{N_m+i+2kN_m}\|_{L^2} + h\|\tilde{\Delta}_v^{N_m+i+2kN_m}\|_{L^2} \right. \right. \\
&\quad \left. \left. + \|\Delta_x^{N_m-i-1+2kN_m}\|_{L^2} + h\|\Delta_v^{N_m-i-1+2kN_m}\|_{L^2} + 4h^2\sqrt{Md} + 2hN_m\sqrt{d} + 2(hN_m)^2\sqrt{Md} \right. \right. \\
&\quad \left. \left. + 2\sqrt{2\gamma}(hN_m)^{3/2}\sqrt{d} \right) \right] \\
&\leq h \sum_{i=0}^{2lN_m-1} \left[\|\delta_v^i\|_{L^2} + hM \left(\|\tilde{\Delta}_x^i\|_{L^2} + h\|\tilde{\Delta}_v^i\|_{L^2} + \|\Delta_x^i\|_{L^2} + h\|\Delta_v^i\|_{L^2} \right) \right] \\
&\quad + 2lh^3MN_m^2\sqrt{d} + 6lh^4N_m^4M\sqrt{Md} + 2\sqrt{2\gamma}lh^{7/2}MN_m^{5/2}\sqrt{d} \\
&\leq h \sum_{i=0}^{2lN_m-1} \left[hM \left(\|\tilde{\Delta}_x^i\|_{L^2} + \|\Delta_x^i\|_{L^2} \right) + (1 + h^2M) \left(\|\tilde{\Delta}_v^i\|_{L^2} + \|\Delta_v^i\|_{L^2} \right) \right] + C_1^X h^3 l N_m.
\end{aligned}$$

Combining components

Therefore combining terms we have that for $l \in \mathbb{N}$ and using the equivalence of norms relation

(3.2) and Proposition 8 we have

$$\begin{aligned}
& \|(\tilde{\Delta}_x^{2lN_m}, \tilde{\Delta}_v^{2lN_m})\|_{L^2, a, b} + \|(\Delta_x^{2lN_m}, \Delta_v^{2lN_m})\|_{L^2, a, b} \leq \|(\delta_x^{2lN_m}, \delta_v^{2lN_m})\|_{L^2, a, b} + 2\|(\Delta_x^{2lN_m}, \Delta_v^{2lN_m})\|_{L^2, a, b} \\
& \leq 2\|\delta_x^{2lN_m}\|_{L^2} + \frac{2}{\sqrt{M}}\|\delta_v^{2lN_m}\|_{L^2} + \frac{6\gamma^2}{M}e^{6\max\{\gamma, \frac{2M}{\gamma}\}hlN_m} \left(\mathbf{C} + \frac{5h^3}{48}(2lN_m + 1) (5M + \gamma M^{1/2}) d^{1/2} \right) \\
& \leq 2h \sum_{i=0}^{2lN_m-1} \left[\left(\frac{C_1^V}{\sqrt{M}} + hM \right) (\|\tilde{\Delta}_x^i\|_{L^2} + \|\Delta_x^i\|_{L^2}) + \left(1 + \frac{hC_1^V}{\sqrt{M}} + h^2M \right) (\|\tilde{\Delta}_v^i\|_{L^2} + \|\Delta_v^i\|_{L^2}) \right] \\
& + 2C_1^X h^3 l N_m + \frac{2}{\sqrt{M}} \left[l N_m h^3 C_2^V + \sqrt{l N_m} h^{5/2} C_3^V \right] \\
& + \frac{6\gamma^2}{M} e^{6\max\{\gamma, \frac{2M}{\gamma}\}hlN_m} \left(\mathbf{C} + \frac{5h^3}{48}(2lN_m + 1) (5M + \gamma M^{1/2}) d^{1/2} \right) \\
& \leq 6h \max \left(\frac{C_1^V}{\sqrt{M}} + hM, \sqrt{M} + hC_1^V + h^2\sqrt{M} \right) \sum_{i=0}^{2lN_m-1} \left[\|(\tilde{\Delta}_x^i, \tilde{\Delta}_v^i)\|_{L^2, a, b} + \|(\Delta_x^i, \Delta_v^i)\|_{L^2, a, b} \right] \\
& + 2C_1^X h^3 l N_m + \frac{2}{\sqrt{M}} \left[l N_m h^3 C_2^V + \sqrt{l N_m} h^{5/2} C_3^V \right] \\
& + \frac{6\gamma^2}{M} e^{6\max\{\gamma, \frac{2M}{\gamma}\}hlN_m} \left(\mathbf{C} + \frac{5h^3}{48}(2lN_m + 1) (5M + \gamma M^{1/2}) d^{1/2} \right) \\
& \leq e^{12hlN_m \max(h\gamma\sqrt{M}N_m + 2\sqrt{M} + hM, \sqrt{M}(1+h^2M+2h\sqrt{M}+h^2\gamma\sqrt{M}N_m))} \left(\mathbf{A}_1 + e^{6\max\{\gamma, \frac{2M}{\gamma}\}hlN_m} \mathbf{A}_2 \right) \\
& \leq e^{12hlN_m(h\gamma\sqrt{M}N_m + 3\sqrt{M})} \left(\mathbf{A}_1 + e^{6\max\{\gamma, \frac{2M}{\gamma}\}hlN_m} \mathbf{A}_2 \right),
\end{aligned}$$

where

$$\begin{aligned}
\mathbf{A}_1 &= \frac{2}{\sqrt{M}} \left[lh^3 N_m^3 \left[\gamma M \left(7 + 2hN_m\sqrt{M} + \sqrt{2\gamma}(hN_m)^{1/2} \right) \sqrt{d} + 18 \left(M_1 d + M\sqrt{Md} \right) \right] \right. \\
& \quad \left. + 14(hN_m)^{5/2} M \sqrt{2l\gamma d} \right] + 4lh^3 M N_m^2 \sqrt{d} + 12lh^4 N_m^4 M \sqrt{Md} + 4\sqrt{2\gamma} l h^{7/2} M N_m^{5/2} \sqrt{d} \\
\mathbf{A}_2 &= \frac{6\gamma^2}{M} \left(\gamma^{-1} N_m l \frac{h^3 \sqrt{d}}{12} \left(3M_1 \sqrt{d} + M^{3/2} + \gamma M \right) + \sqrt{2\gamma^{-1}} \sqrt{\frac{N_m l h^5 M^2 d}{96}} \right. \\
& \quad \left. + \frac{5h^3}{16} l N_m \left(5M + \gamma M^{1/2} \right) d^{1/2} \right).
\end{aligned}$$

□

Lemma 10. *Assuming that $h < \frac{1}{2\gamma}$ and f is M - ∇ Lipschitz and is of the form $f = \sum_{i=1}^{N_m} f_i$, $\gamma \geq \sqrt{8M}$ and each f_i is m_i -strongly convex for $i = 1, \dots, N_m$. Then considering the SMS-UBU scheme with iterates $(x_i, v_i)_{i \in \mathbb{N}}$ defined by Algorithm 2, approximating the continuous dynamics $(X_t, V_t) \in \mathbb{R}^{2d}$ both initialized at the target measure and having synchronously coupled Brownian motion. Then we have if f is M_1 -Hessian Lipschitz that*

$$\|(x_{2lN_m} - X_{2lN_m h}, v_{2lN_m} - V_{2lN_m h})\|_{L^2, a, b} \leq C(\gamma, m, M, M_1, N_m) h^2 d,$$

and if f is M_1^s -strongly Hessian Lipschitz

$$\|(x_{2lN_m} - X_{2lN_m h}, v_{2lN_m} - V_{2lN_m h})\|_{L^2, a, b} \leq C(\gamma, m, M, M_1^s, N_m) h^2 \sqrt{d}.$$

If we impose the stronger stepsize restriction $h < 1/(12\gamma N_m)$, then our bounds simplify to the form

$$\|(x_{2lN_m} - X_{2lN_m h}, v_{2lN_m} - V_{2lN_m h})\|_{L^2, a, b} \leq C(\tilde{\gamma}, \tilde{m}, \tilde{M}, \tilde{M}_1^s) h^2 N_m^{5/2} \sqrt{d},$$

where $\tilde{\gamma} = \gamma/\sqrt{N_m}$, $\tilde{m} = m/N_m$, $\tilde{M} = M/N_m$ and $\tilde{M}_1^s = M_1^s/N_m$.

Proof. Inspired by the interpolation argument used in [38] and also used in [53] we define (x_{2lN_m}, v_{2lN_m}) as $2lN_m$ steps of the SMS-UBU scheme and (X_{2lhN_m}, V_{2lhN_m}) is defined by (2.1) at time $2lhN_m \geq 0$, where these are both initialized at $(X_0, V_0) = (x_0, v_0) \sim \pi$ and have synchronously coupled Brownian motion. We further define a sequence of interpolating variants $(\mathbf{X}_{2lN_m}^{(k)}, \mathbf{V}_{2lN_m}^{(k)})$ for every $k = 0, \dots, l$ all initialized $(\mathbf{X}_0^{(k)}, \mathbf{V}_0^{(k)}) = (\mathbf{X}_0, \mathbf{V}_0)$, where we define $(\mathbf{X}_{2iN_m}^{(k)}, \mathbf{V}_{2iN_m}^{(k)})_{i=1}^k := (X_{2ihN_m}, V_{2ihN_m})_{i=1}^k$ and $(\mathbf{X}_{2iN_m}^{(k)}, \mathbf{V}_{2iN_m}^{(k)})_{i=k+1}^l$ by SMS-UBU steps (each step being a full forward backward sweep) and for $k = l$ we simply have just the continuous diffusion (2.1). Using Proposition 9 we split up the steps into blocks of size \tilde{l} as

$$\begin{aligned} \|(x_{2lN_m} - X_{2lN_m h}, v_{2lN_m} - V_{2lN_m h})\|_{L^2, a, b} &\leq \|(\mathbf{X}_{2lN_m}^{(\lfloor l/\tilde{l} \rfloor)} - \mathbf{X}_{2lN_m h}^{(\lfloor l/\tilde{l} \rfloor)}, \mathbf{V}_{2lN_m}^{(\lfloor l/\tilde{l} \rfloor)} - \mathbf{V}_{2lN_m h}^{(\lfloor l/\tilde{l} \rfloor)})\|_{L^2, a, b} \\ &\quad + \sum_{j=0}^{\lfloor l/\tilde{l} \rfloor - 1} \|(\mathbf{X}_{2lN_m}^{(j\tilde{l})} - \mathbf{X}_{2lN_m h}^{((j+1)\tilde{l})}, \mathbf{V}_{2lN_m}^{(j\tilde{l})} - \mathbf{V}_{2lN_m h}^{((j+1)\tilde{l})})\|_{L^2, a, b}. \end{aligned}$$

Then using the fact that the continuous dynamics preserves the invariant measure and we have contraction of each SMS-UBU forward-backward sweep by Proposition 5 and contraction of each UBU step within each forward-backwards sweep (with different convexity constants). Then we have by considering each term in the previous summation

$$\begin{aligned} &\|(\mathbf{X}_{2lN_m}^{(j\tilde{l})} - \mathbf{X}_{2lN_m h}^{((j+1)\tilde{l})}, \mathbf{V}_{2lN_m}^{(j\tilde{l})} - \mathbf{V}_{2lN_m h}^{((j+1)\tilde{l})})\|_{L^2, a, b} \leq \\ &e^{12h\tilde{l}N_m(h\gamma\sqrt{M}N_m+3\sqrt{M})} \left(\mathbf{A}_1 + e^{6\max\{\gamma, \frac{2M}{\gamma}\}} h\tilde{l}N_m \mathbf{A}_2 \right) \prod_{i=1}^{N_m} \left(1 - \frac{hm_i N_m}{8\gamma} \right)^{2(l-(j+1)\tilde{l})}, \end{aligned}$$

where \mathbf{A}_1 and \mathbf{A}_2 both depend on \tilde{l} . Summing up the terms we get

$$\begin{aligned} \|(x_{2lN_m} - X_{2lN_m h}, v_{2lN_m} - V_{2lN_m h})\|_{L^2, a, b} &\leq \frac{2e^{12h\tilde{l}N_m(h\gamma\sqrt{M}N_m+3\sqrt{M}+\gamma)} (\mathbf{A}_1 + \mathbf{A}_2)}{1 - \prod_{i=1}^{N_m} \left(1 - \frac{hm_i N_m}{8\gamma} \right)^{2\tilde{l}}} \\ &\leq \frac{2e^{12h\tilde{l}N_m(h\gamma\sqrt{M}N_m+3\sqrt{M}+\gamma)} (\mathbf{A}_1 + \mathbf{A}_2)}{1 - e^{-\sum_{i=1}^{N_m} \frac{hm_i N_m \tilde{l}}{4\gamma}}} \\ &\leq 2e^{12h\tilde{l}N_m(h\gamma\sqrt{M}N_m+3\sqrt{M}+\gamma)} (\mathbf{A}_1 + \mathbf{A}_2) \left(1 + \frac{4\gamma}{\sum_{i=1}^{N_m} hm_i N_m \tilde{l}} \right), \end{aligned}$$

due to the fact that $12hN_m(h\gamma\sqrt{M}N_m+3\sqrt{M}) \leq 2$. Firstly considering the larger stepsize regime we consider $\tilde{l} = \lceil \frac{1}{h\gamma} \rceil \leq \frac{2}{h\gamma}$, then

$$\begin{aligned} \|(x_{2lN_m} - X_{2lN_m h}, v_{2lN_m} - V_{2lN_m h})\|_{L^2, a, b} &\leq 2e^{12h\gamma\tilde{l}N_m(h\sqrt{M}N_m+6)} (\mathbf{A}_1 + \mathbf{A}_2) \left(1 + \frac{4\gamma^2}{\sum_{i=1}^{N_m} m_i N_m} \right) \\ &\leq C(\gamma, m, M, M_1^s, N_m) h^2 \sqrt{d}, \end{aligned}$$

or with a d dependence for potentials which are Hessian Lipschitz, but not strongly-Hessian Lipschitz.

If we consider smaller stepsizes, i.e. $h < 1/(12\gamma N_m)$ and choose

$$\tilde{l} = \left\lceil 1/12hN_m(h\gamma\sqrt{M}N_m+3\sqrt{M}+\gamma/2) \right\rceil$$

and using the fact that $\tilde{l} \leq 1/6hN_m(h\gamma\sqrt{M}N_m+3\sqrt{M}+\gamma/2)$ for the considered stepsizes. The right-hand side simplifies to

$$\|(x_{2lN_m} - X_{2lN_m h}, v_{2lN_m} - V_{2lN_m h})\|_{L^2, a, b} \leq C(\gamma/\sqrt{N_m}, m/N_m, M/N_m, M_1^s/N_m) h^2 N_m^{5/2} \sqrt{d},$$

or d rather than \sqrt{d} if the target is Hessian-Lipschitz, but not strongly Hessian Lipschitz. These estimates are uniform in l . \square

Lemma 11. *Considering a potential of the form $f(x) = \sum_{i=1}^{N_m} f_i(x)$, where we assume that f and each f_i for $i = 1, \dots, N_m$ share the same minimizer $x^* \in \mathbb{R}^{2d}$ and each $\nabla^2 f_i \prec M/N_m$ has a M/N_m -Lipschitz gradient, where f is M - ∇ Lipschitz and m -strongly convex we have the following moment bound*

$$\int_{\mathbb{R}^d} \|\nabla f_i(x)\| e^{-f(x)} dx \leq \frac{M}{N_m} \sqrt{\frac{d}{m}}.$$

Proof. Result follows from [43, Lemma 30] and the fact that ∇f_i is Lipschitz with minimizer $x^* \in \mathbb{R}^d$. \square

Remark 8. We do not need to make the assumptions that all the f_i 's have the same minimizer, but we do this to simplify the estimates.

Theorem 12. *Assuming that $h < \frac{1}{2\gamma}$ and f is M - ∇ Lipschitz and is of the form $f = \sum_{i=1}^{N_m} f_i$, $\gamma \geq \sqrt{8M}$ and each f_i is m_i -strongly convex for $i = 1, \dots, N_m$ with minimizer $x^* \in \mathbb{R}^d$. We consider a SMS-UBU scheme with iterates $(x_k, v_k)_{k \in \mathbb{N}}$ defined by Algorithm 2 with stepsize h , approximating the continuous dynamics $(X_t, V_t) \in \mathbb{R}^{2d}$ both with friction parameter γ , initialized at the target measure and having synchronously coupled Brownian motion. Then we have if f is M_1 -Hessian Lipschitz we have that*

$$\|x_k - X_{kh}\|_{L^2} \leq C(\gamma, m, M, M_1, N_m) h^2 d,$$

and if f is M_1^s -strongly Hessian Lipschitz we have that

$$\|x_k - X_{kh}\|_{L^2} \leq C(\gamma, m, M, M_1^s, N_m) h^2 \sqrt{d}.$$

If we impose the stronger stepsize restriction $h < 1/(12\gamma N_m)$, then our bounds simplify to the form

$$\|x_k - X_k\|_{L^2} \leq C(\tilde{\gamma}, \tilde{m}, \tilde{M}, \tilde{M}_1^s) h^2 N_m^{5/2} \sqrt{d},$$

where $\tilde{\gamma} = \gamma/\sqrt{N_m}$, $\tilde{m} = m/N_m$, $\tilde{M} = M/N_m$ and $\tilde{M}_1^s = M_1^s/N_m$, and similarly when we don't assume the potential is strongly Hessian Lipschitz.

Proof. Using Lemma 11 and defining $(\tilde{\Delta}_x, \tilde{\Delta}_v)$ to be the differences in position and velocity between SMS-UBU and the continuous diffusion, one can show that for $k \in \mathbb{N}$

$$\begin{aligned} \|\tilde{\Delta}_v^k\|_{L^2} &\leq \|\tilde{\Delta}_v^{k-1}\|_{L^2} + hM \|y_{k-1} - X_{(k-1/2)h}\|_{L^2} + h\sqrt{Md} + hM\sqrt{\frac{d}{m}} \\ &\leq (1 + h^2M) \|\tilde{\Delta}_v^{k-1}\|_{L^2} + hM \|\tilde{\Delta}_x^{k-1}\|_{L^2} + 3hM\sqrt{\frac{d}{m}}, \end{aligned}$$

and similarly

$$\begin{aligned} \|\tilde{\Delta}_x^k\|_{L^2} &\leq \|\tilde{\Delta}_x^{k-1}\|_{L^2} + h\|\tilde{\Delta}_v^{k-1}\|_{L^2} + h^2M \|y_{k-1} - X_{(k-1/2)h}\|_{L^2} + h^2\sqrt{Md} + h^2M\sqrt{\frac{d}{m}} \\ &\leq (1 + h^2M) \|\tilde{\Delta}_x^{k-1}\|_{L^2} + h(1 + h^2M) \|\tilde{\Delta}_v^{k-1}\|_{L^2} + 3h^2M\sqrt{\frac{d}{m}}. \end{aligned}$$

We then have that

$$\begin{aligned} \|\tilde{\Delta}_x^k\|_{L^2} + \frac{1}{\sqrt{M}} \|\tilde{\Delta}_v^k\|_{L^2} &\leq (1 + 2h\sqrt{M}) \left(\|\tilde{\Delta}_x^{k-1}\|_{L^2} + \frac{1}{\sqrt{M}} \|\tilde{\Delta}_v^{k-1}\|_{L^2} \right) + 5h\sqrt{\frac{Md}{m}} \\ &\leq e^{2h\sqrt{M}k} \left(\|\tilde{\Delta}_x^0\|_{L^2} + \frac{1}{\sqrt{M}} \|\tilde{\Delta}_v^0\|_{L^2} \right) + 5e^{2h\sqrt{M}k} h k \sqrt{\frac{Md}{m}} \end{aligned}$$

and therefore $\|\tilde{\Delta}_v\|_{L^2} \leq \sqrt{M} \left[e^{2h\sqrt{M}k} \left(\|\tilde{\Delta}_x^0\|_{L^2} + \frac{1}{\sqrt{M}} \|\tilde{\Delta}_v^0\|_{L^2} \right) + 5e^{2h\sqrt{M}k} h k \sqrt{\frac{Md}{m}} \right]$.

Therefore

$$\begin{aligned}
\|\tilde{\Delta}_x^k\|_{L^2} &\leq (1 + h^2 M)\|\tilde{\Delta}_x^{k-1}\|_{L^2} + h(1 + h^2 M)\sqrt{M} \left[e^{2h\sqrt{M}k} \left(\|\tilde{\Delta}_x^0\|_{L^2} + \frac{1}{\sqrt{M}}\|\tilde{\Delta}_v^0\|_{L^2} \right) \right] \\
&\quad + 8h^2 k e^{2h\sqrt{M}k} (1 + h^2 M) M \sqrt{\frac{d}{m}} \\
&\leq e^{h^2 M k} \|\tilde{\Delta}_x^0\|_{L^2} + 2e^{3kh\sqrt{M}} \left[hk\sqrt{M} \left(\|\tilde{\Delta}_x^0\|_{L^2} + \frac{1}{\sqrt{M}}\|\tilde{\Delta}_v^0\|_{L^2} \right) + 8(hk)^2 M \sqrt{\frac{d}{m}} \right] \\
&\leq \sqrt{2} e^{h^2 M k} \|(\tilde{\Delta}_x^0, \tilde{\Delta}_v^0)\|_{L^2, a, b} + 4e^{3kh\sqrt{M}} \left[hk\sqrt{M} \|(\tilde{\Delta}_x^0, \tilde{\Delta}_v^0)\|_{L^2, a, b} + 8(hk)^2 M \sqrt{\frac{d}{m}} \right].
\end{aligned}$$

Combining this estimates with Lemma 10 when considering the iterates of SMS-UBU $(x_i, v_i)_{i \in \mathbb{N}}$ approximating (2.1) $(X_t, V_t)_{t \geq 0}$ we have for any $i \in \mathbb{N}$ we can apply the above estimate for $k = i - \lceil \frac{i}{2N_D} \rceil \leq 2N_D$ and then apply Lemma 10 and we have the required result. \square

Theorem 13. *Considering the SG-UBU scheme with friction parameter $\gamma \geq 0$, stepsize $h > 0$, Markov kernel P and initial measure π_0 and assuming that $h < \frac{1}{2\gamma}$, $\gamma \geq \sqrt{8M}$ and the stochastic gradient satisfies Assumptions 1 and 2 with constants C_G and C_{SG} respectively. Let the potential f be M - ∇ Lipschitz, m -strongly convex and of the form $f = \sum_{i=1}^{N_m} f_i$. Then at the k -th iteration we have the non-asymptotic bound*

$$\begin{aligned}
\mathcal{W}_{2, a, b}(\pi_0 P^k, \bar{\pi}) &\leq \left(1 - \frac{mh}{4\gamma} + \frac{5h^2 C_G}{M} \right)^{k/2} \mathcal{W}_{2, a, b}(\pi_0, \bar{\pi}) \\
&\quad + C(\gamma/\sqrt{N_m}, m/N_m, M/N_m, C_G/N_m^2) \left[\frac{C_{SG}\sqrt{h}}{N_m^{1/4}} + h \right] \sqrt{d}.
\end{aligned}$$

Proof. We estimate the difference between the full-gradient UBU scheme and the stochastic gradient scheme UBU scheme initialized at the invariant measure as follows. We use the notation Δ_x^k and Δ_v^k to be the difference in position and velocity at iteration $k \in \mathbb{N}$ respectively. We also use synchronously coupled Brownian motion.

Using (B.4) and (B.7) we have

$$\begin{aligned}
\Delta_v^k &= -h\mathcal{E}(h/2) \sum_{i=1}^k \mathcal{E}(h)^{k-(i-1)} (\nabla f(y_{i-1}) - \mathcal{G}(\tilde{y}_{i-1}, \omega_i)), \\
\Delta_x^k &= \mathcal{F}(h) \sum_{i=1}^{k-1} \Delta_v^i - h\mathcal{F}(h/2) \sum_{i=1}^k (\nabla f(y_{i-1}) - \mathcal{G}(\tilde{y}_{i-1}, \omega_i)).
\end{aligned}$$

Then using independence of the stochastic gradient at each iteration we have and the fact that \mathcal{G} is M -Lipschitz

$$\|(\Delta_x^k, \Delta_v^k)\|_{L^2, a, b} \leq 4h\sqrt{M} \sum_{i=1}^{k-1} \|(\Delta_x^i, \Delta_v^i)\|_{L^2, a, b} + \frac{2h}{\sqrt{M}} \sqrt{\sum_{i=1}^k \|\nabla f(y_{i-1}) - \mathcal{G}(y_{i-1}, \omega_i)\|^2},$$

and using Assumption 2 we have

$$\leq 4h\sqrt{M} \sum_{i=1}^{k-1} \|(\Delta_x^i, \Delta_v^i)\|_{L^2, a, b} + \frac{2h}{\sqrt{M}} \sqrt{\sum_{i=1}^k C_{SG}^2 M^2 \|y_{i-1} - x^*\|^2}.$$

Then using a triangle inequality, the fact that $\|x - x^*\|_{L^2} \leq \sqrt{d/m}$ for $x \sim \pi$, and $\|y_i - X_{(i+1/2)}\|_{L^2} \leq C \frac{\gamma^2}{m} h \sqrt{d}$ by [10, Proposition H.3] we have

$$\begin{aligned} &\leq 4h\sqrt{M} \sum_{i=1}^{k-1} \|(\Delta_x^i, \Delta_v^i)\|_{L^2, a, b} + \frac{Ch}{\sqrt{M}} \sqrt{kC_{SG}^2 M^2 \left(\frac{h^2 \gamma^4 d}{m^2} + \frac{d}{m} \right)} \\ &\leq \frac{Ch}{\sqrt{M}} e^{4hk\sqrt{M}} \sqrt{kC_{SG}^2 M^2 \left(\frac{h^2 \gamma^4 d}{m^2} + \frac{d}{m} \right)}. \end{aligned}$$

Then using interpolation we blocks of size $\lfloor \frac{1}{4h\sqrt{M}} \rfloor$ as we did in Lemma 10 with the Wasserstein convergence result of [59, Proposition B.3.10] we have

$$\begin{aligned} \|(\Delta_x^k, \Delta_v^k)\|_{L^2, a, b} &\leq C \frac{\gamma\sqrt{M}}{m - h\gamma C_G/M} \frac{\sqrt{h}}{\sqrt{M}} \sqrt{\frac{C_{SG}^2 M^2}{\sqrt{M}} \left(\frac{h^2 \gamma^4 d}{m^2} + \frac{d}{m} \right)} \\ &\leq C(\gamma/\sqrt{N_m}, m/N_m, M/N_m, C_G/N_m^2) \frac{C_{SG}\sqrt{hd}}{N_m^{1/4}}, \end{aligned}$$

but we have only bounded the difference between the two schemes and not the diffusion. To conclude the bias estimate we use a triangle inequality with the global error bound for the full-gradient scheme which is a consequence of [10, Proposition H.3]. We also use the contraction results of [59, Proposition B.3.10] in combination with the achieved bias bounds to achieve the non-asymptotic guarantees. \square

Lemma 14. *Let $f : \mathbb{R}^d \rightarrow \mathbb{R}$ of the form $f = \sum_{i=1}^{N_D} f_i$ have an unbiased estimator $\mathcal{G}(\cdot, \omega) = N f_\omega$, where the random variable $\omega \in [N_D]^{N_b}$, then we consider a sequence of random variables $(\omega_i)_{i=1}^{N_m}$ which are sampled uniformly without replacement, where $N_m = N_D/N_b \in \mathbb{N}$. $(x_i)_{i=1}^{N_m}$ are a sequence of random variables which depend on the previous iterate and previous ω . In this setting, we have the estimate*

$$\mathbb{E} \left[\left\| \sum_{i=1}^{N_m} (\mathcal{G}(x_i, \omega_i) - f(x_i)) \right\|^2 \right] \leq \frac{7}{2} \sum_{i=1}^{N_m} \mathbb{E} \left[\|\mathcal{G}(x_i, \omega_i) - f(x_i)\|^2 \right]. \quad (\text{B.10})$$

Proof. Firstly, we expand the square and we consider the cross terms which are of the form $\mathbb{E}[(f(x_i) - \mathcal{G}(x_i, \omega_i))(f(x_j) - \mathcal{G}(x_j, \omega_j))]$ for $i \neq j$. Let $\omega'_j = \omega_j$ with probability $1 - \frac{1}{N_m}$, and $\omega'_j = \omega_i$ with probability $\frac{1}{N_m}$. Then it is easy to see that ω'_j is uniformly distributed on the set $\{1, \dots, N_m\}$, independently of ω_i . As a consequence

$$\begin{aligned} &\mathbb{E}[(f(x_i) - \mathcal{G}(x_i, \omega_i))(f(x_j) - \mathcal{G}(x_j, \omega_j))] = \mathbb{E}[(f(x_i) - \mathcal{G}(x_i, \omega_i))(f(x_j) - \mathcal{G}(x_j, \omega'_j))] \\ &\quad + \mathbb{E}[(f(x_i) - \mathcal{G}(x_i, \omega_i))((f(x_j) - \mathcal{G}(x_j, \omega_j)) - (f(x_j) - \mathcal{G}(x_j, \omega'_j)))] , \end{aligned}$$

then the first term has zero expectation. The second term can be written as

$$\begin{aligned} &\mathbb{E}[(f(x_i) - \mathcal{G}(x_i, \omega_i))((f(x_j) - \mathcal{G}(x_j, \omega_j)) - (f(x_j) - \mathcal{G}(x_j, \omega'_j))) \mathbb{1}[\omega_j \neq \omega_{j'}]] \leq \\ &\frac{1}{2} \mathbb{E} \left[(f(x_i) - \mathcal{G}(x_i, \omega_i))^2 \mathbb{1}[\omega_j \neq \omega_{j'}] \right] \\ &\quad + \frac{1}{2} \mathbb{E} \left[((f(x_j) - \mathcal{G}(x_j, \omega_j)) \mathbb{1}[\omega_j \neq \omega_{j'}] - (f(x_j) - \mathcal{G}(x_j, \omega'_j)) \mathbb{1}[\omega_j \neq \omega_{j'}])^2 \right] \\ &\leq \frac{1}{2N_m} \mathbb{E} \left[(f(x_i) - \mathcal{G}(x_i, \omega_i))^2 \right] + \frac{1}{N_m} \mathbb{E} \left[(f(x_j) - \mathcal{G}(x_j, \omega_j))^2 + (f(x_j) - \mathcal{G}(x_j, \omega'_j))^2 \right], \end{aligned}$$

and summing up the terms we have the required result. \square

Proof of Theorem 7. We estimate the difference between the full-gradient UBU scheme and the stochastic gradient scheme UBU scheme as follows. We use the notation Δ_x^k and Δ_v^k to be the difference in position and velocity at iteration $k \in \mathbb{N}$ respectively. We also use synchronously coupled Brownian motion.

Using (B.4) and (B.7) we have

$$\begin{aligned} \Delta_v^k &= \mathcal{E}(h)^k \Delta_v^0 - h\mathcal{E}(h/2) \sum_{i=1}^k \mathcal{E}(h)^{k-(i-1)} (\nabla f(y_{i-1}) - N_m \nabla f_{\omega_{i+1}}(\tilde{y}_{i-1})) \\ &= \mathcal{E}(h)^k \Delta_v^0 - h\mathcal{E}(h/2) \sum_{i=0}^{\lfloor \frac{k}{2N_m} \rfloor - 1} \sum_{j=0}^{2N_m-1} \mathcal{E}(h)^{k-1-2iN_m-j} (\nabla f(y_{2N_m i+j}) - N_m \nabla f_{\omega_{2iN_m+j+1}}(\tilde{y}_{2iN_m+j})) \\ &\quad - h\mathcal{E}(h/2) \sum_{i=2N_m \lfloor k/2N_m \rfloor}^k \mathcal{E}(h)^{k-i} (\nabla f(y_{i-1}) - N_m \nabla f_{\omega_{i+1}}(\tilde{y}_{i-1})), \end{aligned}$$

and therefore using the fact that the ω_i random variables are independent between each block of size $2N_m$ and applying Lemma 14 to the forward and backward sweeps individually we have the following L^2 estimate

$$\|\Delta_v^k\|_{L^2} \leq \|\Delta_v^0\|_{L^2} + \sum_{i=0}^{k-1} hM \|y_i - \tilde{y}_i\|_{L^2} + \sqrt{7}h\mathcal{E}(h/2) \sqrt{\sum_{i=0}^{k-1} \|\nabla f(y_i) - N_m \nabla f_{\omega_{i+1}}(y_i)\|_{L^2}^2}.$$

Considering x we similarly have

$$\|\Delta_x^k\|_{L^2} \leq \|\Delta_x^0\|_{L^2} + \sum_{i=0}^{k-1} [h^2M \|y_i - \tilde{y}_i\|_{L^2} + h\|\Delta_v^i\|_{L^2}] + \sqrt{7}h^2 \sqrt{\sum_{i=0}^{k-1} \|\nabla f(y_i) - N_m \nabla f_{\omega_{i+1}}(y_i)\|_{L^2}^2},$$

and therefore if they are initialized at the same point we can combine the estimates and get

$$\begin{aligned} \|(\Delta_x^k, \Delta_v^k)\|_{L^2, a, 0} &\leq 4h\sqrt{M} \sum_{i=0}^{k-1} \|(\Delta_x^i, \Delta_v^i)\|_{L^2, a, 0} + \frac{2\sqrt{7}h}{\sqrt{M}} \sqrt{\sum_{i=0}^{k-1} \|\nabla f(y_i) - N_m \nabla f_{\omega_{i+1}}(y_i)\|_{L^2}^2} \\ &\leq 4h\sqrt{M} \sum_{i=0}^{k-1} \|(\Delta_x^i, \Delta_v^i)\|_{L^2, a, 0} + 2\sqrt{7}h\sqrt{M}C_{SG} \sqrt{\sum_{i=0}^{k-1} \|y_i - X_{(i+1/2)h}\|_{L^2}^2 + k\frac{d}{m}}, \end{aligned}$$

where we have used that $\|x - x^*\|_{L^2} \leq \sqrt{d/m}$ for $x \sim \pi$. By using that $\|y_i - X_{(i+1/2)h}\|_{L^2} \leq C\frac{2}{m}h\sqrt{d}$ (see [10, Proposition H.3]) we have

$$\begin{aligned} &\leq 4h\sqrt{M} \sum_{i=0}^{k-1} \|(\Delta_x^i, \Delta_v^i)\|_{L^2, a, 0} + Ch\sqrt{M}C_{SG} \sqrt{k\frac{\gamma^4}{m^2}h^2d + k\frac{d}{m}} \\ &\leq Ch\sqrt{M}C_{SG}e^{4hk\sqrt{M}} \sqrt{kd\left(\frac{\gamma^4}{m^2}h^2 + \frac{1}{m}\right)}. \end{aligned}$$

Now doing interpolation as in the proof of Theorem 13 with blocks of size $\lfloor 1/4h\sqrt{M} \rfloor$ we have the required estimate when we combine the result with [10, Proposition H.3] and use contraction of the UBU scheme at each step with different convexity constants $(m_i)_{i=1}^{N_m}$. \square

C Further details on numerical experiments

Pytorch code for neural network of Fashion-MNIST example:

```

in_channels: int = 3
num_classes: int = 2
flattened_size: int = 16384
low_rank: int = 32

self.conv_layer = nn.Sequential(
    # Conv Layer block 1
    nn.Conv2d(in_channels=in_channels, out_channels=32, kernel_size=3, padding=1),
    nn.Softplus(beta=1.0),
    nn.BatchNorm2d(32,momentum=1.0),
    nn.Conv2d(in_channels=32, out_channels=64, kernel_size=3, padding=1),
    nn.Softplus(beta=1.0),
    nn.MaxPool2d(kernel_size=2, stride=2),
    nn.BatchNorm2d(64,momentum=1.0),
    # Conv Layer block 2
    nn.Conv2d(in_channels=64, out_channels=64, kernel_size=3, padding=1),
    nn.Softplus(beta=1.0),
    nn.BatchNorm2d(64,momentum=1.0),
    nn.Conv2d(in_channels=64, out_channels=128, kernel_size=3, padding=1),
    nn.Softplus(beta=1.0),
    nn.BatchNorm2d(128,momentum=1.0),
    nn.Conv2d(in_channels=128, out_channels=128, kernel_size=3, padding=1),
    nn.MaxPool2d(kernel_size=2, stride=2),
    # Conv Layer block 3
    nn.BatchNorm2d(128,momentum=1.0),
    nn.Conv2d(in_channels=128, out_channels=256, kernel_size=3, padding=1),
    nn.Softplus(beta=1.0),
    nn.BatchNorm2d(256,momentum=1.0),
    nn.Conv2d(in_channels=256, out_channels=256, kernel_size=3, padding=1),
    nn.Softplus(beta=1.0),
    nn.MaxPool2d(kernel_size=2, stride=2),
)

self.fc_layer = nn.Sequential(
    nn.Flatten()
    nn.BatchNorm1d(flattened_size,momentum=1.0),
    nn.Linear(flattened_size, low_rank),
    nn.BatchNorm1d(low_rank,momentum=1.0),
    nn.Linear(low_rank,512),
    nn.Softplus(beta=1.0),
    nn.BatchNorm1d(512,momentum=1.0),
)

self.last_layer=nn.Sequential(
    nn.Linear(512, num_classes)
)

```

Pytorch code for neural network of hair colour (blonde/brown) classification on Celeb-A dataset:

```

in_channels: int = 3
num_classes: int = 2
flattened_size: int = 16384
low_rank: int = 16

self.conv_layer = nn.Sequential(

```

```

# Conv Layer block 1
nn.Conv2d(in_channels=in_channels, out_channels=32, kernel_size=3, padding=1),
nn.Softplus(beta=1.0),
nn.BatchNorm2d(32, momentum=1.0),
nn.Conv2d(in_channels=32, out_channels=64, kernel_size=3, padding=1),
nn.Softplus(beta=1.0),
nn.MaxPool2d(kernel_size=2, stride=2),
nn.BatchNorm2d(64, momentum=1.0),
# Conv Layer block 2
nn.Conv2d(in_channels=64, out_channels=128, kernel_size=3, padding=1),
nn.Softplus(beta=1.0),
nn.BatchNorm2d(128, momentum=1.0),
nn.Conv2d(in_channels=128, out_channels=128, kernel_size=3, padding=1),
nn.Softplus(beta=1.0),
nn.MaxPool2d(kernel_size=2, stride=2),
nn.BatchNorm2d(128, momentum=1.0),
# Conv Layer block 3
nn.Conv2d(in_channels=128, out_channels=256, kernel_size=3, padding=1),
nn.Softplus(beta=1.0),
nn.BatchNorm2d(256, momentum=1.0),
nn.Conv2d(in_channels=256, out_channels=256, kernel_size=3, padding=1),
nn.Softplus(beta=1.0),
nn.MaxPool2d(kernel_size=2, stride=2),
)

self.fc_layer = nn.Sequential(

    nn.BatchNorm1d(flattened_size, momentum=1.0),
    nn.Linear(flattened_size, low_rank),
    nn.BatchNorm1d(low_rank, momentum=1.0),
    nn.Linear(low_rank, 4096),
    nn.Softplus(beta=1.0),
    nn.BatchNorm1d(4096, momentum=1.0),
    nn.Linear(4096, low_rank),
    nn.BatchNorm1d(low_rank, momentum=1.0),
    nn.Linear(low_rank, 1024),
    nn.Softplus(beta=1.0),
    nn.BatchNorm1d(1024, momentum=1.0),
    nn.Linear(1024, low_rank),
    nn.BatchNorm1d(low_rank, momentum=1.0),
    nn.Linear(low_rank, 512),
    nn.Softplus(beta=1.0),
    nn.BatchNorm1d(512, momentum=1.0),
)

self.last_layer=nn.Sequential(
    nn.Linear(512, num_classes)
)

```

Pytorch code for neural network of Chest X-ray example:

```

in_channels: int = 1
num_classes: int = 2
flattened_size: int = 12544
low_rank: int = 32

```

```

self.conv_layer = nn.Sequential(
    nn.Conv2d(in_channels=in_channels, out_channels=32, kernel_size=3, stride=1, padding=1),
    nn.Softplus(beta=1.0),
    nn.MaxPool2d(kernel_size=2, stride=2, padding=1),
    # Second Convolutional Block
    nn.BatchNorm2d(32,momentum=1.0),
    nn.Conv2d(in_channels=32, out_channels=64, kernel_size=3, stride=1, padding=1),
    nn.Softplus(beta=1.0),
    nn.MaxPool2d(kernel_size=2, stride=2, padding=1),
    # Third Convolutional Block
    nn.BatchNorm2d(64,momentum=1.0),
    nn.Conv2d(in_channels=64, out_channels=64, kernel_size=3, stride=1, padding=1),
    nn.Softplus(beta=1.0),
    nn.MaxPool2d(kernel_size=2, stride=2, padding=1),
    # Fourth Convolutional Block
    nn.BatchNorm2d(64,momentum=1.0),
    nn.Conv2d(in_channels=64, out_channels=128, kernel_size=3, stride=1, padding=1),
    nn.Softplus(beta=1.0),
    nn.MaxPool2d(kernel_size=2, stride=2, padding=1),
    # Fifth Convolutional Block
    nn.BatchNorm2d(128,momentum=1.0),
    nn.Conv2d(in_channels=128, out_channels=256, kernel_size=3, stride=1, padding=1),
    nn.Softplus(beta=1.0),
    nn.MaxPool2d(kernel_size=2, stride=2, padding=1),
)

self.fc_layer = nn.Sequential(
    nn.Flatten()
    nn.BatchNorm1d(flattened_size,momentum=1.0),
    nn.Linear(flattened_size, low_rank),
    nn.BatchNorm1d(low_rank,momentum=1.0),
    nn.Linear(low_rank, 512),
    nn.Softplus(beta=1.0),
    nn.BatchNorm1d(512,momentum=1.0),
)

self.last_layer=nn.Sequential(
    nn.Linear(512, num_classes)
)

```

Our hyperparameter choices are stated in Table 2.

Dataset	Initial L.R.	SWA L.R.	Stepsize h	ρ	ρ_{\max}	Friction γ
Fashion-MNIST	10^{-2}	10^{-3}	$2.5 \cdot 10^{-4}$	$50^{-1/2}$	$6 \cdot 50^{-1/2}$	ρ^{-1}
Celeb-A(blonde/brun.)	10^{-2}	10^{-3}	$2.5 \cdot 10^{-4}$	0.2	$6 \cdot 0.2$	ρ^{-1}
Chest X-ray	10^{-2}	10^{-3}	$5 \cdot 10^{-4}$	$50^{-1/2}$	$6 \cdot 50^{-1/2}$	ρ^{-1}

Table 2: Details about the datasets and neural networks used in our experiments

References

- [1] Zapatero Alfonso Álamo. *Word Series for the Numerical Integration of Stochastic Differential Equations*. PhD thesis, Universidad de Valladolid, 2021.
- [2] Christoph Andrieu, Nando De Freitas, Arnaud Doucet, and Michael I. Jordan. An introduction to MCMC for machine learning. *Machine learning*, 50(1):5–43, 2003.
- [3] Jack Baker, Paul Fearnhead, Emily B. Fox, and Christopher Nemeth. Control variates for stochastic gradient MCMC. *Stat. Comput.*, 29(3):599–615, 2019.
- [4] Carlo Baldassi, Fabrizio Pittorino, and Riccardo Zecchina. Shaping the learning landscape in neural networks around wide flat minima. *Proceedings of the National Academy of Sciences*, 117(1):161–170, 2020.
- [5] Neil Band, Tim G. J. Rudner, Qixuan Feng, and et al. Benchmarking Bayesian deep learning on diabetic retinopathy detection tasks. *Neural Information Processing Systems (NeurIPS) 2021 Datasets and Benchmarks Track Proceedings*, 2021.
- [6] Rémi Bardenet, Arnaud Doucet, and Chris Holmes. On Markov chain Monte Carlo methods for tall data. *The Journal of Machine Learning Research*, 18(47):1–43, 2017.
- [7] Christopher M Bishop and Nasser M Nasrabadi. *Pattern recognition and machine learning*, volume 4. Springer, 2006.
- [8] Charles Blundell, Julien Cornebise, Koray Kavukcuoglu, and Daan Wierstra. Weight uncertainty in neural network. In *International conference on machine learning*, pages 1613–1622. PMLR, 2015.
- [9] Nawaf Bou-Rabee and Houman Owhadi. Long-run accuracy of variational integrators in the stochastic context. *SIAM J. Numer. Anal.*, 48(1):278–297, 2010.
- [10] Neil K. Chada, Benedict Leimkuhler, Daniel Paulin, and Peter A. Whalley. Unbiased kinetic Langevin Monte Carlo with inexact gradients. *arXiv preprint arXiv:2311.05025*, 2023.
- [11] Martin Chak and Pierre Monmarché. Reflection coupling for unadjusted generalized Hamiltonian Monte Carlo in the nonconvex stochastic gradient case. *arXiv preprint arXiv:2310.18774*, 2023.
- [12] Niladri Chatterji, Nicolas Flammarion, Yian Ma, Peter Bartlett, and Michael Jordan. On the theory of variance reduction for stochastic gradient Monte Carlo. In *International Conference on Machine Learning*, pages 764–773. PMLR, 2018.
- [13] Tianqi Chen, Emily Fox, and Carlos Guestrin. Stochastic gradient Hamiltonian Monte Carlo. In *International Conference on Machine Learning*, page 1683–1691, 2014.
- [14] Yifan Chen, Xiaou Cheng, Jonathan Niles-Weed, and Jonathan Weare. Convergence of Unadjusted Langevin in High Dimensions: Delocalization of Bias. *arXiv preprint arXiv:2408.13115*, 2024.
- [15] Yuansi Chen and Khashayar Gatmiry. When does Metropolized Hamiltonian Monte Carlo provably outperform Metropolis-adjusted Langevin algorithm? *arXiv preprint arXiv:2304.04724*, 2023.
- [16] Xiang Cheng, Niladri S Chatterji, Peter L Bartlett, and Michael I Jordan. Underdamped Langevin MCMC: A non-asymptotic analysis. In *Conference on learning theory*, pages 300–323. PMLR, 2018.
- [17] Adam D. Cobb and Brian Jalaian. Scaling Hamiltonian Monte Carlo inference for Bayesian neural networks with symmetric splitting. *Proceedings of the Thirty-Seventh Conference on Uncertainty in Artificial Intelligence*, 161:675–685, 2021.

- [18] Anthony Costa Constantinou and Norman Elliott Fenton. Solving the problem of inadequate scoring rules for assessing probabilistic football forecast models. *Journal of Quantitative Analysis in Sports*, 8(1), 2012.
- [19] Miles Cranmer, Daniel Tamayo, Hanno Rein, Peter Battaglia, Samuel Hadden, Philip J Armitage, Shirely Ho, and David N. Spergel. A Bayesian neural network predicts the dissolution of compact planetary systems. *PNAS*, 118(40), 2021.
- [20] Arnak S. Dalalyan and Avetik Karagulyan. User-friendly guarantees for the Langevin Monte Carlo with inaccurate gradient. *Stochastic Process. Appl.*, 129(12):5278–5311, 2019.
- [21] Arnak S. Dalalyan and Lionel Riou-Durand. On sampling from a log-concave density using kinetic Langevin diffusions. *Bernoulli*, 26(3):1956–1988, 2020.
- [22] Michael Dusenberry, Ghassen Jerfel, Yeming Wen, Yian Ma, Jasper Snoek, Katherine Heller, Balaji Lakshminarayanan, and Dustin Tran. Efficient and scalable Bayesian neural nets with rank-1 factors. In *International Conference on Machine Learning*, pages 2782–2792, 2020.
- [23] Andreas Eberle, Arnaud Guillin, and Raphael Zimmer. Couplings and quantitative contraction rates for Langevin dynamics. *Ann. Probab.*, 47(4):1982–2010, 2019.
- [24] Pierre Foret, Ariel Kleiner, Hossein Mobahi, and Behnam Neyshabur. Sharpness-aware minimization for efficiently improving generalization. In *International Conference on Learning Representations*, 2021.
- [25] Nicholas Geneva and Nicholas Zabaras. Modeling the dynamics of PDE systems with physics-constrained deep auto-regressive networks. *Journal of Computational Physics*, 403(109056), 2020.
- [26] Michael B. Giles, Mateusz B. Majka, Lukasz Szpruch, Sebastian J. Vollmer, and Konstantinos C. Zygalakis. Multi-level Monte Carlo methods for the approximation of invariant measures of stochastic differential equations. *Stat. Comput.*, 30(3):507–524, 2020.
- [27] Nicolai Gouraud, Pierre Le Bris, Adrien Majka, and Pierre Monmarché. HMC and underdamped Langevin united in the unadjusted convex smooth case. *arXiv preprint arXiv:2202.00977*, 2022.
- [28] Alan M Horowitz. A generalized guided Monte Carlo algorithm. *Physics Letters B*, 268(2):247–252, 1991.
- [29] Pavel Izmailov, Dmitrii Podoprikin, Timur Garipov, Dmitry Vetrov, and Andrew Gordon Wilson. Averaging weights leads to wider optima and better generalization. 34th Conference on Uncertainty in Artificial Intelligence 2018, pages 876–885, 2018.
- [30] Pavel Izmailov, Sharad Vikram, Matthew D. Hoffman, and Andrew G. Wilson. What are Bayesian neural network posteriors really like? In *Proceedings of the 38th International Conference on Machine Learning*, 139:4629–4640, 2021.
- [31] Daniel S Kermany, Michael Goldbaum, Wenjia Cai, Carolina CS Valentim, Huiying Liang, Sally L Baxter, Alex McKeown, Ge Yang, Xiaokang Wu, Fangbing Yan, et al. Identifying medical diagnoses and treatable diseases by image-based deep learning. *cell*, 172(5):1122–1131, 2018.
- [32] Mohammad Khan, Didrik Nielsen, Voot Tangkaratt, Wu Lin, Yarin Gal, and Akash Srivastava. Fast and scalable Bayesian deep learning by weight-perturbation in ADAM. In *International Conference on Machine Learning*, 161:675–685, 2021.
- [33] Dow-Mu Koh, Nickolas Papanikolaou, Ulrich Bick, and et al. Artificial intelligence and machine learning in cancer imaging. *Commun Med*, 2022.

- [34] Ben Leimkuhler, Akash Sharma, and Michael V Tretyakov. Numerical integrators for confined langevin dynamics. *arXiv preprint arXiv:2404.16584*, 2024.
- [35] Benedict Leimkuhler and Charles Matthews. Rational construction of stochastic numerical methods for molecular sampling. *Appl. Math. Res. Express. AMRX*, (1):34–56, 2013.
- [36] Benedict Leimkuhler, Charles Matthews, and Gabriel Stoltz. The computation of averages from equilibrium and nonequilibrium Langevin molecular dynamics. *IMA J. Numer. Anal.*, 36(1):13–79, 2016.
- [37] Benedict Leimkuhler, Daniel Paulin, and Peter A Whalley. Contraction rate estimates of stochastic gradient kinetic Langevin integrators. *arXiv preprint arXiv:2306.08592*, page 4, 2023.
- [38] Benedict J. Leimkuhler, Daniel Paulin, and Peter A. Whalley. Contraction and convergence rates for discretized kinetic Langevin dynamics. *SIAM J. Numer. Anal.*, 62(3):1226–1258, 2024.
- [39] Jesse Levinson and et al. Towards fully autonomous driving: Systems and algorithms. *Intelligent Vehicles Symposium (IV)*, pages 163–168, 2011.
- [40] David J. C. MacKay. Probable networks and plausible predictions — a review of practical Bayesian methods for supervised neural networks. *Network: computation in neural systems*, 6(3):469–505, 1995.
- [41] Wesley J Maddox, Pavel Izmailov, Timur Garipov, Dmitry P Vetrov, and Andrew Gordon Wilson. A simple baseline for bayesian uncertainty in deep learning. *Advances in neural information processing systems*, 32, 2019.
- [42] RV Mises and Hilda Pollaczek-Geiringer. Praktische verfahren der gleichungsauflösung. *ZAMM-Journal of Applied Mathematics and Mechanics/Zeitschrift für Angewandte Mathematik und Mechanik*, 9(1):58–77, 1929.
- [43] Pierre Monmarché. High-dimensional MCMC with a standard splitting scheme for the under-damped Langevin diffusion. *Electron. J. Stat.*, 15(2):4117–4166, 2021.
- [44] Radford M. Neal. *Bayesian Learning for Neural Networks*. Springer Science & Business Media, 2012.
- [45] Christopher Nemeth and Paul Fearnhead. Stochastic gradient Markov chain Monte Carlo. *Journal of the American Statistical Association*, 116(533):433–450, 2021.
- [46] Jeremy Nixon, Michael W. Dusenberry, Linchuan Zhang, Ghassen Jerfel, and Dustin Tran. Measuring calibration in deep learning. In *Proceedings of the IEEE/CVF Conference on Computer Vision and Pattern Recognition (CVPR) Workshops*, June 2019.
- [47] Theodore Papamarkou, Jacob Hinkle, Todd Young, and David Womble. Challenges in Markov chain Monte Carlo for Bayesian neural networks. *Statistical Science*, 37(3):435–442, 2022.
- [48] Daniel Paulin and Peter A. Whalley. Correction to “Wasserstein distance estimates for the distributions of numerical approximations to ergodic stochastic differential equations”. *arXiv preprint arXiv: arXiv:2402.08711*, 2024.
- [49] Grigorios A Pavliotis. Stochastic processes and applications. *Texts in applied mathematics*, 60, 2014.
- [50] Herbert Robbins and Sutton Monro. A stochastic approximation method. *The Annals of Mathematical Statistics*, pages 400–407, 1951.

- [51] Jesus Maria Sanz-Serna and Konstantinos C Zygalakis. Wasserstein distance estimates for the distributions of numerical approximations to ergodic stochastic differential equations. *J. Mach. Learn. Res.*, 22:242–1, 2021.
- [52] Katharina Schuh. Global contractivity for Langevin dynamics with distribution-dependent forces and uniform in time propagation of chaos. *Ann. Inst. Henri Poincaré Probab. Stat.*, 2024.
- [53] Katharina Schuh and Peter A Whalley. Convergence of kinetic langevin samplers for non-convex potentials. *arXiv preprint arXiv:2405.09992*, 2024.
- [54] Inass Sekkat and Gabriel Stoltz. Quantifying the mini-batching error in Bayesian inference for adaptive Langevin dynamics. *J. Mach. Learn. Res.*, 24:Paper No. [329], 58, 2023.
- [55] Li Shen, Yan Sun, Zhiyuan Yu, Ding Liang, Xinmei Tian, and Dacheng Tao. On Efficient Training of Large-Scale Deep Learning Models: A Literature Review. *arXiv preprint arxiv:2304.03589*, 2023.
- [56] Hiral Thadeshwar, Vinit Shah, Mahek Jain, Rujata Chaudhari, and Vishal Badgajar. Artificial intelligence based self-driving car. : *2020 4th International Conference on Computer, Communication and Signal Processing (ICCCSP)*, 2020.
- [57] Sebastian J. Vollmer, Konstantinos C. Zygalakis, and Yee Whye Teh. Exploration of the (non-)asymptotic bias and variance of stochastic gradient Langevin dynamics. *J. Mach. Learn. Res.*, 17:Paper No. 159, 45, 2016.
- [58] Max Welling and Yee Whye Teh. Bayesian learning via stochastic gradient Langevin dynamics. In *Proceedings of the 28th International Conference on Machine Learning*, pages 681–688, 2011.
- [59] Peter Archibald Whalley. *Kinetic Langevin Monte Carlo methods*. PhD thesis, The University of Edinburgh, 2024.
- [60] Han Xiao, Kashif Rasul, and Roland Vollgraf. Fashion-MNIST: a novel image dataset for benchmarking machine learning algorithms. *arXiv preprint arXiv:1708.07747*, 2017.
- [61] Shuo Yang, Ping Luo, Chen-Change Loy, and Xiaoou Tang. From facial parts responses to face detection: A deep learning approach. In *Proceedings of the IEEE international conference on computer vision*, pages 3676–3684, 2015.
- [62] Ruqi Zhang, Chunyuan Li, Jianyi Zhang, Changyou Chen, and Andrew G. Wilson. Cyclical stochastic gradient MCMC for Bayesian deep learning. In *International Conference on Learning Representations*, 2020.